Molecular Pharmacology Fast Forward. Published on August 6, 2020 as DOI: 10.1124/mol.120.119412
This article has not been copyedited and formatted. The final version may differ from this version.

Title: Dietary caffeine synergizes adverse peripheral and central responses to anesthesia in malignant hyperthermia susceptible mice

Authors: Monica Aleman[†@], Rui Zhang[†], Wei Feng, Lihong Qi, Jose R. Lopez[§], Chelsea Crowe, Yao Dong, Genady Cherednichenko, and Isaac N. Pessah[*@]

Author Affiliations: RZ, WF, JRL, YD, GC, INP: Department of Molecular Biosciences, School of Veterinary Medicine, University of California, Davis, CA 95616, USA;
MA, CC: Department of Medicine and Epidemiology, The William R. Pritchard Veterinary Medical Teaching Hospital, School of Veterinary Medicine, University of California, Davis, CA 95616, USA; LQ: Department of Public Health Sciences, School of Medicine, School of Medicine, University of California, Davis, CA 95616, USA

Molecular Pharmacology Fast Forward. Published on August 6, 2020 as DOI: 10.1124/mol.120.119412
This article has not been copyedited and formatted. The final version may differ from this version.

Running title: Dietary caffeine exacerbates MH susceptibility

Number of text pages: 49

Number of tables: 1

Number of figures: 7

Number of references: 78

Number of words in Abstract: 250

Number of words in Introduction: 1012

Number of words in Discussion: 1483

Nonstandard abbreviations in alphabetical order: ADR Adverse Drug Response, BLM Bilayer lipid membrane, Bza Benzotriazole, CAF Caffeine, DAN Dantrolene, ECG Electrocardiogram, EEG Electroencephalogram, EEG_{TP}, EEG total power (μV); FMH, filament MH; HAL Halothane, HET Mice heterozygous for R163C-RYR1, i.p. intraperitoneal; IVCT In vitro contracture test, MH Malignant hyperthermia, MHS MH susceptible, Po Open probability, RYR1 Ryanodine receptor type 1, RYR2 Ryanodine receptor type 2, SR/ER Sarcoplasmic/endoplasmic reticulum, VEH Vehicle, WT Wildtype

Molecular Pharmacology Fast Forward. Published on August 6, 2020 as DOI: 10.1124/mol.120.119412
This article has not been copyedited and formatted. The final version may differ from this version.

Abstract

Ryanodine receptor (*RYR*) mutations confer stress-triggered malignant hyperthermia susceptibility (MHS). Dietary caffeine (CAF) is the most commonly consumed psychoactive compound by humans. CAF-triggered Ca^{2+} release and its influences on skeletal muscle contractility are widely used as experimental tools to study RYR function/dysfunction and diagnose MHS. We hypothesize that dietary CAF achieving blood levels measured in human plasma exacerbates the penetrance of *RYR1* MHS mutations triggered by gaseous anesthetic, affecting both central and peripheral adverse responses. Heterozygous R163C-RYR1 MHS mice (HET) are used to investigate the influences of dietary CAF on both peripheral and central responses before and after induction of halothane maintenance anesthesia (HAL) under experimental conditions that maintain normal core body temperature. HET receiving CAF (plasma CAF 893ng/ml) have significantly shorter times to respiratory arrest compared to WT, without altering blood chemistry, displaying hyperthermia or muscle rigor. Bolus dantrolene i.p. (DAN) before HAL prolongs time to respiratory arrest. A pilot electrographic study using subcutaneous electrodes reveals that dietary CAF does not alter baseline EEG total power, but significantly shortens delay to isoelectric EEG, which precedes respiratory and cardiac arrest. CAF±HAL are studied on RYR1 single-channel currents and HET myotubes to define molecular mechanisms of gene-by-environment synergism. Strong pharmacological synergism between CAF and HAL is demonstrated in both single channel and myotube preparations. Central and peripheral nervous systems mediate adverse responses to HAL in a HET model of MHS exposed to dietary CAF, a modifiable lifestyle factor that may mitigate risks of acute and chronic diseases associated with *RYR1* mutations.

Significance Statement

Dietary caffeine at a human-relevant dose synergizes adverse peripheral and central responses to anesthesia in malignant hyperthermia susceptible mice. Synergism of these drugs can be attributed to their actions at ryanodine receptors.

Molecular Pharmacology Fast Forward. Published on August 6, 2020 as DOI: 10.1124/mol.120.119412
This article has not been copyedited and formatted. The final version may differ from this version.

Introduction

Mutations in the gene that encodes ryanodine receptor type 1 (*RYR1*) are known to cause fulminant malignant hyperthermia (MH), an acute, potentially fatal, pharmacogenetic disease triggered perioperatively by the use of halogenated volatile anesthetics or depolarizing muscle relaxants (Zhou 2014). Clinical manifestations of a fulminant crisis include extreme hypercapnia, metabolic and respiratory acidosis, hyperlactatemia, hyperthermia, profuse sweating, tachycardia, tachypnea, muscle rigidity, and ultimately death (Litman et al. 2018; Zhou 2014). In food and companion animals (Aleman et al. 2004; Fujii et al. 1991; McCarthy et al. 1990; Roberts et al. 2001), as well as murine models that express human MH susceptibility mutations in *RYR1*, exertional and environmental heat stress is also known to trigger a fulminant MH crisis (Chelu et al. 2006; Lopez et al. 2018; Yang et al. 2006; Yuen et al. 2012). Patients with mutations within *RYR1* and 20 additional loci are linked to susceptibility to myopathic injury throughout the lifespan (Jungbluth et al. 2018). However, the clinical onset and severity of histopathological damage vary broadly among individual mutation carriers and their relationship to *RYR1* genotype is complex, suggesting medical, lifestyle and environmental factors may contribute not only to the initiation of fulminant MH during the perioperative period but also enhanced susceptibility to the promotion of chronic myopathic injury through unknown mechanisms (Rosenberg et al. 2015; Voermans et al. 2016).

MH susceptibility is generally viewed through the lens of rare skeletal muscle diseases with the clinical diagnosis of MH susceptibility relying on *in vitro* contracture testing (IVCT) performed on skeletal muscle biopsies from suspected probands to

Molecular Pharmacology Fast Forward. Published on August 6, 2020 as DOI: 10.1124/mol.120.119412
This article has not been copyedited and formatted. The final version may differ from this version.

ascertain enhanced sensitivity to caffeine (CAF) and halothane (HAL) induced muscle contracture (Hopkins et al. 2015). Although a strong linkage exists with the *RYR1* locus on chromosome 19, the large number of expressed genomic *RYR1* variants (>300) known to occur in the human population, as well as suggestive linkage with 6 additional loci, has made genetic screening impractical as a first-line diagnosis (Hopkins et al. 2015). As such, the IVCT remains the gold standard for the diagnosis of MH in human medicine (Hopkins et al. 2015; Litman et al. 2018; Zhou 2014). When feasible, a positive IVCT is confirmed by genetic screening of the *RYR1* locus. Recent estimates of *RYR1* genotype-phenotype (IVCT) concordance range as low as 34% in Australian studies (Gillies et al. 2008; Gillies et al. 2015), to 52% in a US study (Brandom et al. 2013) to as high as 76% in a primarily European Caucasian cohort drawn from the UK (Miller et al. 2018). However, results from a recent multicenter case control study of 229 genotype-positive subjects with previously recorded exposure to trigger anesthetics found an overall penetrance for the analyzed *RYR1* mutations of only 40.6% (Ibarra Moreno et al. 2019). Lower than expected genotype-phenotype concordance, including discordance within a family between a functionally relevant *RYR1* variant and the IVCT phenotype, has been attributed to low penetrance of many *RYR1* variants in the absence of other genetic risk factors or errors in either genotyping or phenotyping (Adeokun et al. 1997; Miller et al. 2018; Robinson et al. 2003), or non-genetic risk factors, such as age and sex (Ibarra Moreno et al. 2019).

Considering the pharmacogenetic nature of MH susceptibility and our dependence of its diagnosis on muscle sensitivity to CAF and/or HAL (i.e., the IVCT), whether human-relevant plasma concentrations of dietary CAF may or may not influence adverse drug

responses (ADR) *in vivo* has not been previously considered. CAF is the most widely consumed psychoactive compound worldwide, with 85% of US adults consuming an average intake of 200-400 mg/day, mainly through caffeinated beverages (Barone and Roberts 1996; Mitchell et al. 2014). An English study of 600 medical outpatients reported a mean plasma caffeine concentration of 2.1 mg/l (10.9 μM) (Smith et al. 1982) which is consistent with more recent levels measured in US nonsmokers (9.9 to 17.4 μM) and smokers (2.8 to 10.1 μM), levels that are positively correlated with consumption (de Leon et al. 2003). In the latter study, 99% of study participants have detectable caffeine with a mean caffeine intake of 3.02 mg/kg/day. Although CAF consumption through diet has generally been considered safe to human health, recent studies with animal models and from human epidemiology suggest possible adverse influences on genetically susceptible populations (Cornelis et al. 2006; Ding et al. 2014; Findley et al. 2019; Korekar et al. 2019; Palatini et al. 2009; Yang et al. 2010; Zhou and Hypponen 2019).

Here, we address three biologically interrelated questions using *in vivo* exposures, cellular imaging and single-channel voltage clamp approaches to assess the influences of dietary CAF at levels well within those currently measured in plasma of human populations worldwide can influence the penetrance of MH susceptibility to volatile gaseous anesthetic such as HAL and its currently used alternatives. We hypothesize that dietary CAF achieving blood levels measured in human plasma exacerbates the penetrance of *RYR1* MHS mutations triggered by gaseous anesthetic, affecting both central and peripheral adverse responses. We further address whether DAN, currently the standard of care treatment to mitigate the onset and progression of fulminant MH (Rosen et al. 2019), will mitigate the synergistic effects of CAF during anesthesia. Using the heterozygous R163C MH susceptible mouse model (HET), one of the more common

Molecular Pharmacology Fast Forward. Published on August 6, 2020 as DOI: 10.1124/mol.120.119412
This article has not been copyedited and formatted. The final version may differ from this version.

mutations confirmed to cause MH susceptibility in humans, herein we provide direct evidence that dietary CAF profoundly influences both peripheral and central cortical responses that are synergistic to those of HAL. Compared to wildtype mice, MH susceptible mice show different basal EEG total power (EEG_{TP}) in the absence and presence of dietary CAF, and the CAF exposed HET show shorter times to achieve isoelectric EEG, respiratory and cardiac arrest under HAL anesthesia in the absence of fulminant hyperthermia or muscle rigidity. The synergism between CAF and HAL is demonstrated in myotubes *in vitro* and can be directly attributed to their synergistic influences on alteration of RYR1 channel function.

These results are the first to identify peripheral and central nervous system contributions to MH susceptibility and demonstrate that a common modifiable lifestyle factor, caffeine consumption, significantly modifies the penetrance of a common *RYR1* mutation.

Molecular Pharmacology Fast Forward. Published on August 6, 2020 as DOI: 10.1124/mol.120.119412
This article has not been copyedited and formatted. The final version may differ from this version.

Materials and Methods

Animals for *in vivo* studies: All animal dosing, terminal experiments, euthanasia, and tissue and blood collection procedures were conducted under protocols approved by the Institutional Animal Care and Use Committee (IACUC# 18094) at the University of California, Davis (Davis, CA). All animals were C57BL6/J maintained in a vivarium with constant temperature and humidity with a 12:12 light-dark cycle. Animals were provided with Mouse Diet 20 (PicoLab) and autoclaved drinking water provided by UC Davis animal facility ad libitum. Well-trained, certified staff were responsible for the periodic time-mating of breeding R163C-RYR1 heterozygous (HET) and wildtype (WT) trios and provided mice *in vivo* experiments. All the animal related procedures met the requirements of the guidelines of Animal Use and Care of the National Institutes of Health and approved by the UC Davis Animal Use and Care Committee.

Two separate cohorts of adult mice (4 to 6 months of age) were used for *in vivo* dietary caffeine studies. Both male and female wild type (WT) and R163C-RYR1 heterozygous (HET) mice were included in the dietary caffeine studies either receiving vehicle (+VEH; water) or dietary caffeine (+CAF) with (+DAN) or without (-DAN) a single dose of dantrolene (2.5 mg/kg i.p.) prior to commencing anesthesia. HET mice were generated with a knock-in mutation-targeting vector as described previously, and bred into the C57BL/6 background (The Jackson Laboratory) after the genotype was confirmed (Yang et al. 2006; Cherednichenko et al. 2008; Feng et al. 2011; Giulivi et al. 2011; Truong and Pessah 2019).

For the main study which monitored respiration (**Cohort 1**), 10-16 mice were randomly assigned to one of eight treatment groups as follows: WT+VEH (n=13),

Molecular Pharmacology Fast Forward. Published on August 6, 2020 as DOI: 10.1124/mol.120.119412
This article has not been copyedited and formatted. The final version may differ from this version.

WT+CAF (n=16), HET+VEH (n=13), HET+CAF (n=14), HET+VEH+DAN (n=11), HET+CAF+DAN (n=10). Approximately 50% males and females were included in each group. Additional mice were randomly assigned to four treatment groups (WT+VEH; WT+CAF; HET+VEH; HET+CAF) to measure possible influences of the dietary CAF protocol on Baseline blood chemistry without subjecting then to maintenance HAL.

A follow-on pilot study with a smaller number of mice (**Cohort 2**) was undertaken to replicate findings in **Cohort 1** using electrographic monitoring. Power analysis based on effect sizes obtained with **Cohort 1** indicated an n=3 to 4 mice per treatment/genotype group was sufficient to ascertain temporal differences across genotype and treatment groups for cortical EEG, respiratory rate and heart rate with an 80% chance of a $p=0.05$. Mice were randomly assigned to six treatment groups as follows: WT+VEH (n=3), WT+CAF (n=3), HET+VEH (n=3), HET+CAF (n=3), HET+VEH+DAN (n=3), HET+CAF+DAN (n=4) and instrumented for electrographic recordings as described below.

Chemicals and solutions: Caffeine (CAF; ≥99.0%, CAS 58-08-2) and halothane (HAL; 2-bromo-2-chloro-1,1,1-trifluoroethane, ≥99.0%, CAS 151-67-7) were obtained from Sigma-Aldrich (St. Louis, MO). Dantrolene sodium (Dantrium Intravenous, CAS 14663-23-1; DAN) was obtained as a lyophilized mixture with mannitol and sodium hydroxide from Ben Venue Laboratories (Bedford, OH). Solutions of 0.05% HAL (4.75 mM), in the presence or absence of CAF, were prepared from a neat stock (9.5 M containing 0.01% thymol) diluted 1:2000 in Locke's buffer immediately before each cellular experiment. All solutions were kept in sealed amber tubes protected from light. For single channel voltage clamp experiments, CAF, HAL or the combination were made as 10X working stocks in

Molecular Pharmacology Fast Forward. Published on August 6, 2020 as DOI: 10.1124/mol.120.119412
This article has not been copyedited and formatted. The final version may differ from this version.

amber tubes and introduced directly into the *cis* chamber solution (see below). All dilution stocks were made and used on the day of each experiment. All HAL solutions were thoroughly dissolved in buffer with sonication before use.

Oral CAF dosing and blood levels: Using the assumption that the average human weighs 70 kg and the average mouse weighs 25 g, this daily intake is equivalent to 0.143 mg/day in mice based on a 400 mg daily intake in humans, equivalent to 5.7 mg/kg/day in mice. Following Kleiber's law (Kleiber 1947), which states that an organism's total metabolic rate is equal to the ¾ power of its mass, and accordingly, its specific metabolic rate (metabolic rate per unit of mass) is equal to the -¼ power of its mass, we calculated that a 25 g mouse is ~7.2 times more metabolically active compared to a 70 kg human. Pilot studies were performed to identify a CAF p.o. dose that would result in blood levels similar to those measured in human blood of CAF consumers based on the mean daily CAF intake of 200-400 mg reported previously by others (Barone and Roberts 1996; de Leon et al. 2003; Mitchell et al. 2014; Smith et al. 1982). Therefore, adjusting for allometric and metabolic differences and assuming a mouse drinks 5 mL of water a daily, we defined the target dose of 0.2 mg/mL of CAF in drinking water. Mice were maintained on vehicle (VEH) or CAF ad libitum for ≥7 d to ensure a steady-state CAF concentration in the circulation. Both VEH and CAF dosing solutions were filtered through 0.2 μm filters after preparation. For both genotypes, mice were randomly assigned to receive either VEH (5% sucrose in water) or CAF (0.2 mg/mL with 5% sucrose in water) through drinking water.

All plasma samples (standards and unknowns) were processed together to ensure

consistency and to minimize errors. Fresh stocks of caffeine and benzotriazole were prepared in ultrapure water. Using caffeine-free plasma pooled from a set of naïve mice, standards were created by spiking samples of the blank plasma (100 μL each) with known concentrations of caffeine (0-250 μM). All standards and unknowns (100 μL each) were then spiked with the internal standard benzotriazole (50 μM). Two volumes of ethyl acetate were added to the samples and vortexed for 10 min, followed by centrifugation at 10,000 x *g* for 10 min. Samples were placed in -80°C to quickly freeze the aqueous phase and the organic layer was collected. The remaining aqueous phase was extracted a second time using the same protocol described above. The organic phase was pooled from the two extractions and evaporated under gentle heat (35-40°C) on a dry heat block in the fume hood. The remaining residue was reconstituted in 100 μL of the mobile phase (ultrapure water with 0.1% acetic acid) by vigorous mixing.

High-performance liquid chromatography (HPLC) system used consisted of a Waters (Milford, MA) 510 HPLC Pump, Waters 717plus Autosampler, and Waters 2487 Dual λ Absorbance Detector controlled using Empower Pro software (Waters). The mobile phase (phase A) was ultrapure water with 0.1% acetic acid, and the organic phase (phase B) was acetonitrile with 0.1% acetic acid; all phases were degassed by vacuum filtration. Reconstituted samples (40 μL) were injected onto a C_{12} Synergi 4 μm Max-RP 80 Å (250 x 4.6 mm) LC column (Phenomenex, Torrance, CA) with a guard column. The flow rate was set at 1 mL/min using the following linear gradient protocol:

Time (min)	% A	% B
0	100	0
30	50	50
35	0	100
40	100	0
55	100	0

Samples were monitored using the absorbance module at λ = 273 nm. Retention time ratios between CAF and internal standard benzotriazole were consistent between injections. For each sample, the ratio between the CAF peak AUC (AUC_{CAF}) and benzotriazole peak AUC (AUC_{Bza}) was calculated. A standard curve was developed using known CAF concentrations and their respective AUC_{CAF}:AUC_{Bza} ratio, and unknowns were calculated using this linear regression.

Anesthesia protocols: For the main study (**Cohort 1**), mice were briefly anesthetized with HAL delivered in a plastic induction chamber with 2.0% HAL in medical air (vol/vol) for ≤ 2 min and transferred prone on a Peltier thermostatic platformed. A rectal probe was inserted with feedback control to the platform to maintain the core body temperature of each mouse between 35-37°C to prevent fulminant hyperthermia (elevated core temperature and hypercontraction). Maintenance at 1.5% HAL (vol/vol) continued for up to 45 min delivered through a nosecone. HAL (1.5% vol/vol) was used for maintenance anesthesia because it approximates one minimum alveolar concentration (MAC) or the anesthetic EC50 value. In clinical practice, patients are exposed to 0.5 - 1.3 MAC. Respiration was monitored visually and time to respiratory arrest scored with the observer blinded to treatment group. Analysis of these data failed to show sex differences and the data were combined for analysis. Statistical comparisons of percent survival across groups was based on loss respiration using Kaplan-Meier survival analyses followed by a log-rank/Mantel-Cox test (GraphPad Prism Software, La Jolla, CA with $p < 0.05$ considered significant).

For the electrographic pilot study (**Cohort 2**) mice were lightly pre-anesthetized with i.p. 10 mg xylazine hydrochloride and 100 mg ketamine hydrochloride 10 minutes to accommodate placement of subcutaneous needle electrodes prior to initiating maintenance HAL anesthesia as described above. Electrographic electrodes were placed to obtain simultaneous recordings of EEG, respiratory rate and ECG before (Baseline period) and after commencing maintenance anesthesia with 1.5% HAL though a nosecone (Maintenance period). In order to determine the possible influences of dantrolene sodium (DAN) on HET mice without or with dietary CAF, a separate set of HET mice without (HET+VEH; n = 3) or with (HET+CAF; n = 4) were injected with i.p. 2.5 mg/kg DAN 20 minutes prior to commencing the placement of EEG electrodes, as described above. Data was continuously acquired for 10 min before initiation of maintenance anesthesia to simultaneously monitor baseline EEG, respiration, ECG and core body temperature patterns (Baseline period). Once 10 min of baseline data were acquired, mice were maintained with 1.5% HAL (vol/vol in medical air) through a nosecone (Maintenance period) while continuously recording EEG, respiration, ECG, and core temperature for the duration of the experiment which lasted up to 60 min for WT groups or until heart rate became undetectable (HET groups).

Electroencephalographic study details: Electroencephalogram (EEG), respiratory and electrocardiogram (ECG) were recorded simultaneously with a Nihon Kohden digital wireless EEG system (Irvine, CA) with continuous video monitoring. Electrode location and names were according to the International 10-20 system and are depicted in **Supplemental Fig S1** (Klem et al. 1999) A transverse bipolar montage was selected. Recording channels were placed in the central region and included: left aural to the left

Molecular Pharmacology Fast Forward. Published on August 6, 2020 as DOI: 10.1124/mol.120.119412
This article has not been copyedited and formatted. The final version may differ from this version.

central (A_1-C_3), left central to central vertex (C_3-Cz), central vertex to right central (Cz-C_4), and right central to right aural (C_4-A_2). These central regions were selected because they were least affected by artifacts in the event of movement; thus, quantitative analysis was limited to this configuration (Williams et al. 2008). Two electrodes for the recording of ECG were placed subcutaneously on the left side at the level of the base and apex of the heart (**Supplemental Fig S1**). Twelve consecutive 10-second epochs of recording were also selected immediately before commencing 1.5% HAL anesthesia (defined as Baseline Period), and 3 consecutive 10-seconds epochs every 5 minutes thereafter until the end of the study defined as the Maintenance period (45 minutes for WT mice, at cessation of a detectable heart beat for MH susceptible mice). Standard quantitative EEG values (power in each frequency band, total power, median frequency, spectral edge (95%), and suppression ratio were calculated and additional analysis such as evaluation of paroxysmal activity was performed and statistically analyzed (Origin Pro 9; OriginLab, MA). Paroxysmal activity included spikes (duration <70 ms), sharp waves (70-<200 ms), and spike-and-slow waves (>200 ms).

For both Baseline and Maintenance periods, epochs were visually examined using a transverse bipolar montage (Kochs et al. 1993). Each epoch was processed with software that used a fast Fourier transform analysis (FFT) for calculation of peak frequency and power, plus absolute power (μV^2) in each frequency band (Hz) (Kochs et al. 1993). Frequency band definition consisted of δ (>0-<4 Hz), θ (4-<8), α (8-<13), β (13-<30), and γ (>30). Total power (all bands combined) was calculated from these data. Frequency (Hz) and amplitude (μV) were also calculated.

Linear mixed effects models (Laird et al., 1982; Fitzmaurice et al., 2004) were

employed to determine the difference in the Baseline EEG total power and normalized EEG total reduction fraction during the HAL Maintenance period among the treatment groups. For the baseline EEG total power, discrete time and treatment were used as fixed effects to investigate influences in mean EEG total power and random intercept for mouse to account for the correlation between the repeated measurements for each mouse over time. For the Maintenance phase of the study, normalized EEG total reduction fraction, discrete time, treatment and time*treatment interaction were included as fixed effects to describe the mean effects of these factors. Random intercepts for mouse and time nested within mouse were used to account for the correlations between the repeated measurements for the same mouse over time and multiple measurements from each mouse at each time, respectively. Pairwise post-hoc testing was performed and multiple comparisons for the main effects of treatment were corrected by the Tukey-Kramer (Kramer 1956) method for unbalanced data. Due to the large number of pairwise comparisons performed for the interaction of treatment*time, the false discovery rate (FDR) (Benjamini and Hochberg, 1995) method was applied for multiple testing correction, reflecting the nature of this pilot study whose primary aim is to generate hypotheses for future larger scale studies, and some false positive is acceptable. The FDR procedure has greater power than some more conservative methods such as the Bonferroni correction, which was also generated as a sensitivity analysis. Mixed effects models were conducted using SAS 9.4 Proc Mixed, and, and the FDR procedure and the Bonferroni correction were performed using Proc Multtest (SAS Institute, Cary, NC) and an adjusted P value < 0.05 was considered statistically significant.

Clinical chemistry analysis: Blood was collected from a separate set of VEH- or CAF-exposed WT and HET mice to analyze baseline clinical chemistry in the absence of HAL anesthesia to obtain a reference baselines and determine possible genotype differences to dietary CAF. Additional WT and HET mice were subjected to the maintenance HAL protocol described above maintaining core temperature. A additional group of HET mice were subjected to the same HAL protocol but core temperatures were permitted to rise freely to 39-40°C at which time they triggered with at fulminant MH episode characterized by generalized rigor of the limbs and tail as previously reported (Yang et al. 2006; Cherednichenko et al. 2008; Feng et al. 2011; Giulivi et al. 2011; Truong and Pessah 2019;), at which time blood was collected.

For all animals, blood was collected by blind cardiac puncture using a syringe with a 25-gauge needle; the needle was inserted below the xiphoid process of the sternum through the diaphragm with a slight bias to the right to target the apex of the heart. Mice were exsanguinated through this process, which provided up to 1 mL of whole blood; all animals were cervically dislocated after exsanguination. Blood was stored at 4°C in BD Vacutainer tubes treated with heparin with gel separator (BD, Franklin Lakes, NJ). Plasma was separated by centrifugation at 2,000 x g for 10 min at 4°C. Samples were delivered fresh on ice to the Veterinary Medicine Teaching Hospital Clinical Diagnostic Laboratory Services at UC Davis for analysis.

Blood chemistry parameters were sorted into the following categories: electrolytes (sodium, potassium, calcium, magnesium, chloride) and pH (anion gap, bicarbonate). Data were analyzed using a one-way ANOVA with Tukey's post-test.

Molecular Pharmacology Fast Forward. Published on August 6, 2020 as DOI: 10.1124/mol.120.119412
This article has not been copyedited and formatted. The final version may differ from this version.

Measurement of RYR1 single-channel activity in bilayer lipid membrane: RYR1 single channels from junctional SR prepared from WT animals were incorporated by inducing fusion of junctional SR vesicles with a planar bilayer lipid membrane (BLM) composed of 30 mg/mL phosphatidylethanolamine-phosphatidylserine-phosphatidylcholine (Avanti Polar Lipids, Alabaster, Alabama; 5:3:2 w/w in decane). BLM formed across a 200 μm apparatus partitioned two sides that were defined as *cis* (cytoplasmic) and *trans* (luminal) sides of the channel. Both *cis* and *trans* chambers were filled with solutions buffered by 20 mM HEPES at pH 7.4. RyR1 containing membrane vesicles were added to the *cis* chamber, which was defined as the cytoplasmic side. Test compounds (CAF and/or HAL) were added from freshly prepared 10x stocks to the *cis* chamber containing 500 mM CsCl and 2 μM free Ca^{2+} adjusted by EGTA according to the software Bound and Determined (Brooks and Storey 1992). The *cis* side served as virtual ground. The *trans* chamber was held at -40 mV contained 50 mM CsCl and 100 μM Ca^{2+}. Single-channel gating activity was recorded, filtered at 1 kHz (Low-Pass Bessel Filter 8 Pole, Warner Instruments, Hamden, CT) before being acquired through Digidata 1320A and AxoScope 10 software (Molecular Devices, Sunnyvale, CA). Analysis of single-channel open probability (P_o), mean open dwelling time constant (τ) was calculated using pClamp 9 software (Molecular Devices). All single-channel recordings were made at ambient 23-25 °C.

pClamp 9 software was used to capture and analyze single channel gating kinetics. OriginLab 9.1 (Northampton, MA, USA), Prism GraphPad 8 (San Diego, CA, USA) and were used for statistical analysis and plotting graphs. The detailed methods for sampling sizes and statistical analysis are described under results and specifically

indicated in each figure legend. All statistical analyses/inter-group comparisons were specified ($p \leq 0.05$) before any data were obtained, and outcomes of all performed statistical tests are reported, irrespective of *p* values actually obtained.

Preparation and culture of primary skeletal myoblasts: Primary skeletal myoblasts were isolated from neonatal WT and R163C (HET) mice, as described previously in (Beam and Knudson 1988; Rando and Blau 1994). Myoblasts were grown in cell culture treated dishes coated with calfskin collagen (Sigma-Aldrich) in Ham's F-10 medium containing 20% (vol/vol) bovine growth serum (HyClone, GE Healthcare Life Sciences, Logan, UT), 2 mM L-glutamine, penicillin G, streptomycin sulfate, and 4 ng/mL fibroblast growth factor (Peprotech, Rocky Hill, NJ) at 37°C in 5% CO_2 and 10% O_2. For Ca^{2+} imaging experiments, cells were plated onto 96-well μClear plates (Corning Life Sciences, Tewksbury, MA) coated with Matrigel (Corning Life Sciences). Upon reaching ~80% confluence, the cells were differentiated into myotubes over a period of 3-4 days in DMEM containing 5% (vol/vol) heat-inactivated horse serum, 2 mM L-glutamine, penicillin G, and streptomycin sulfate at 37°C in 5% CO_2 and 10% O_2. All recordings were made at ambient 23-25^{o}C. Myotubes were loaded with Fluo-4 and imaged using an inverted microscope as previously described (Feng et al., 2011). Drug applications, singly or in combinations, were performed using a closed perfusion system driven by peristaltic pumps at a constant flow rate of 2.5 ml/min interspersed with 2 min of washout with buffer between drug applications. All HAL containing reservoir solutions were sealed and shielded from light.

All data represent mean ± SE. $^{*}p \leq 0.05$, comparing between genotypes at each CAF concentration (One-way ANOVA with Bonferroni's post-test, using OriginLab 9.0).

Results

Dietary CAF significantly shortens time to respiratory arrest of HET mice without influencing basal blood chemistry: Mice exposed to caffeine (CAF, 0.2 mg/mL) through drinking water for 7 or more days achieved a median plasma CAF concentration of 893 ng/ml (4.6 μM) at the time they were exposed to anesthesia and did not differ between genotypes (**Fig 1C**; Trough). Considering the relatively abbreviated CAF half-life in mice (Hartmann and Czok 1980) and the nocturnal behavior of these animals, we sought to estimate the pharmacokinetic peak achieved through our dosing scheme by collecting blood at nighttime from a separate set of animals. From ten samples collected in this manner, the Peak median CAF concentration was 25.6 μM (**Fig 1C**; Peak). The Trough and Peak values serve as estimators of the CAF concentration range available to deliver to systemic organs, including skeletal muscle and brain. These levels are within the target range of the median human plasma concentrations of CAF in developed countries (Smith et al. 1982; Barone and Roberts 1996; de Leon et al. 2003; Mitchell et al. 2014).

Despite achieving the desired levels of plasma CAF concentrations in mice, CAF did not influence Baseline blood chemistry biomarkers for electrolytes, pH, renal, or liver function compared to the non-caffeinated group (**Supplemental Table S1**; first 4 columns). Furthermore, there were no significant genotype-specific differences in the absence or presence of dietary CAF (**Supplemental Table S1**; first 4 columns). Thus, dietary levels of CAF achieved in the present study do not significantly alter blood chemistry readings across genotypes under baseline conditions.

A separate cohort of WT and HET mice (**Cohort 1**) were assigned to treatment

Molecular Pharmacology Fast Forward. Published on August 6, 2020 as DOI: 10.1124/mol.120.119412
This article has not been copyedited and formatted. The final version may differ from this version.

groups with and without CAF exposure to test the hypothesis that dietary CAF attaining blood levels measured in human plasma exacerbates the penetrance of *RYR1* MHS mutations triggered by gaseous anesthetic. In sharp contrast to basal blood biomarkers, ventilation with 1.5% (vol/vol) HAL resulted in significant shortening in survival time (time to respiratory arrest) in HET mice receiving dietary CAF compared to HET mice receiving VEH (**Fig 2 and Table insert** *p=0.0026*). The median time to respiratory arrest during maintenance anesthesia for HET mice dosed with VEH was 14.5 min, whereas HET mice exposed to dietary CAF had a median survival time of 10.5 min. Although the loss of respiration was also observed with WT mice in the VEH (1 of 13 tested) and CAF (3 of 16 tested) exposed groups at 45 min, survival was not significantly different between WT treatment groups (p = 0.60, Mantel-Cox).

DAN inhibits RYR1 channels activity and is currently the standard of care for MH (Ratto and Joyner 2019; Rosen et al. 2019). As shown in the **Fig 2 and Table insert**, Dantrolene (DAN; 2.5 mg/kg i.p.) administered 20 min prior to HAL anesthesia of HET significantly prolonged median times to respiratory arrest in both VEH- and CAF-exposed HET groups; -CAF from 14.5 to 30 min (*p=0.0007*) and +CAF from 10.5 to 24 min (*p<0.0001).* DAN treatment also eliminated the influence of dietary CAF (-CAF+DAN vs. +CAF+DAN; p = 0.3820) while reducing the steepness of the survival curves for both treatment groups such that respiratory arrest occurred over a broader span of time (**Fig 2**).

Dietary CAF does not alter Baseline cortical EEG but reduces time to isoEEG during HAL Maintenance period: Given that dietary CAF significantly shortens time to lethal

Molecular Pharmacology Fast Forward. Published on August 6, 2020 as DOI: 10.1124/mol.120.119412
This article has not been copyedited and formatted. The final version may differ from this version.

outcome (respiratory arrest) with HAL anesthesia (**Fig 2**) in the absence of fulminant hyperthermia or measurable alterations in blood chemistry, we conducted a pilot study with mice instrumented for electrographic recording (**Cohort 2**; **Supplemental Fig S2**). This approach provides an independent means to monitor central (EEG) and peripheral (respiration rate and ECG) responses to HAL in real-time. Since respiratory arrest triggered by 1.5% HAL anesthesia occurred in the absence of hyperthermia and muscle rigidity characteristic of a fulminant MH episode, we analyzed cortical EEG total power (EEG_{TP}), respiratory rate and ECG rate simultaneously to assess possible differences across genotype and treatment groups. During the initial Baseline period, prior to commencing maintenance anesthesia with 1.5% HAL, WT and HET mice failed to show significant differences in EEG total power (μV) whether or not they received dietary CAF (data not shown).

The electrographic protocol used during maintenance anesthesia also incorporated feedback cooling to maintain core body temperature between 35-37^{o}C, which precluded the onset of acute hyperthermia (**Fig 3A**) typically associated with the fulminant MH episode in HET mouse line (Yang et al. 2006; Feng et al. 2011). Nevertheless, HAL anesthesia proved lethal to HET mice and review of video recordings indicated the absence of muscle twitches, nor did they exhibit signs of skeletal muscle contracture or flexion of the limbs and tail at the time of respiratory and cardiac arrest (data not shown). Mice were flaccid at the time of death and remained so until rigor mortis set in >30 min postmortem. All WT mice in the **Cohort 2** study recovered from anesthesia regardless of CAF exposure. In contrast, HET mice sequentially lost detectable respiration and ECG with mean latencies of 14.4$\pm$0.8 and 24.2$\pm$5.2 min, respectively (**Fig**

3B, C). HET mice exposed to dietary CAF had a 29% shorter time to respiratory arrest (*p=0.005*), with cardiac arrest also showing 29% shorter mean time although not reaching statistical significance, likely due to large variability in the measurement (**Fig 3B, C**). HET mice receiving DAN (2.5 mg/kg i.p.) 20 min before initiating HAL anesthesia had 2.3 to 2.7-fold longer time to respiratory arrest (*p<0.05*; **Fig 3B**) regardless of CAF treatment. DAN also prolonged the time to loss of ECG in HET mice exposed to VEH 1.6-fold (*p<0.05*), although the differences in respective latencies did not reach significance in mice receiving dietary CAF (**Fig 3C**).

Blood samples collected from a subset of **Cohort 2** HET mice at the time of death (HET+VEH) or at an equivalent time from (WT+VEH) showed modestly elevated plasma potassium (128%) and magnesium (116%), whereas anion gap and phosphorus were elevated 177% and 196%, respectively, indicating moderate acidosis associated with an adverse metabolic response at the time of death compared to plasma samples collected from WT mice subjected to the same HAL protocol (**Supplemental Table S1**; WT+CAF+HAL *vs*. HET+CAF+HAL - No FMH, i.e., no fulminant MH achieved). A separate group of mice was subjected to the same HAL anesthesia protocol with the exception that their core body temperature was not clamped within the normal physiological range (no feedback cooling was applied), rather they were permitted to progress to fulminant hyperthermia and generalized skeletal muscle contracture as previously described (Chelu et al. 2006; Yang et al. 2006; Yuen et al. 2012). HET mice with fulminant MH (FMH) had significantly elevated plasma sodium (109%), potassium (206%) and calcium (140%), magnesium (136%), phosphorous (290%) and an elevated anion gap (280%) and reduced bicarbonate (48%) compared to WT control, indicating

Molecular Pharmacology Fast Forward. Published on August 6, 2020 as DOI: 10.1124/mol.120.119412
This article has not been copyedited and formatted. The final version may differ from this version.

severe acidosis and hyperkalemia at the time of death (**Supplemental Table S1**, WT+CAF+HAL (No FMH) *vs*. HET+CAF+HAL (FMH).

The temporal change in EEG_{TP} during the HAL Maintenance period was further analyzed as the reduction fraction normalized to the Baseline EGG_{TP} measured for each mouse. **Figure 4** summarizes the temporal patterns in EEG_{TP} throughout the Maintenance phase. Although mice in WT+VEH and WT+CAF showed a modest decline in EEG_{TP} during the Maintenance period, neither time nor treatment were significantly different (**Fig 4A**). In contrast, HET mice displayed significant progressive declines in EGG_{TP} during Maintenance period with HAL reaching isoEEG within 35 minutes (**Fig 4B**) regardless of CAF exposure. However, HET mice exposed to dietary CAF showed significantly shorter temporal decrements to isoEEG than HET exposed to vehicle alone (adjusted P=0.025; **Fig 4** Table insert). Interventions with DAN prior to commencing the Maintenance period did not significantly alter the decay fraction compared to HET+VEH and was not influenced by dietary CAF (compare HET vs HET+DAN or HET+CAF+DAN; adjusted P>0.05; **Fig 4** Table insert). However, DAN selectively eliminated the effects of dietary CAF exposure by delaying the fractional reduction in EEG_{TP} (compare HET+CAF+DAN vs HET+DAN (adjusted P=0.64) or HET+CAF (adjusted P=0.0008). Noteworthy was the highly significant differences in the loss of EEG_{TP} in HET+DAN vs HET+CAF treatment groups (Adjusted P<0.0001; **Fig 4B** and Table insert).

Further results of the influences of time*treatment interactions revealed that, once controlled for false discovery rate, the most significant differences between HET+VEH vs HET+CAF occurred within the first 10 min of the Maintenance phase of HAL anesthesia (Supplemental **Table S2**). In comparison, the influence of DAN was to prolong EEG_{TP} throughout the recording time in animals exposed to dietary CAF (Supplemental **Table S2**).

Molecular Pharmacology Fast Forward. Published on August 6, 2020 as DOI: 10.1124/mol.120.119412
This article has not been copyedited and formatted. The final version may differ from this version.

VEH-treated HET mice rapidly lost detectable cortical brainwave activity, achieving isoEEG with a mean time of 12.3 ± 1.9 min. Mean time to isoEEG preceded the mean time to loss of ECG (50% shorter time), regardless whether mice received VEH or dietary CAF (-CAF group: mean time from 12.3 ± 1.9 to 24.2 ± 5.2 min, p=0.018; and +CAF group: mean latency from 8.9 ± 0.8 to 17.2 ± 4.8 min, p<0.036, respectively) (**Table 1**). At the time cortical EEG activity was lost, there was no evidence of alterations on ECG morphology such as absent P wave, wide QRS, or tall T (not shown), indicating that modest hyperkalemia observed at this time (**Supplement Table 1**) was insufficient to affect changes in ECG.

Synergism of HAL and CAF towards RYR1 single-channel function: We next tested the hypothesis that CAF and HAL, in combination, produce synergistic effects on RYR1 channels, their putative molecular target. Functional RYR1 channels assemble as homotetramers. Tissues from HET mice would be expected to produce WT/HET chimeric channels of all possible ratios resulting in heterogenous channel behaviors even in the presence of tightly defined *cis/trans* buffer solutions (Feng et al. 2011). To circumvent confounding issues that arise due to channel heterogeneity, and the fact that the combination of HAL+CAF significantly synergizes responses in WT myotubes (see **Fig 7**, below), we investigated whether the combination was capable of directly synergizing single-channel kinetics isolated from WT RYR1. Accordingly, skeletal muscle junctional SR (JSR) fused with bilayer lipid membranes (BLM) in order to measure single-channel gating kinetics under voltage clamp. The exemplary baseline gating activity of WT RYR1 channels (two channels were incorporated in the BLM) in the presence of 2 μM:100 μM *cis*:*trans* Ca^{2+} exhibited low P_o that increased 21-fold upon addition of the combination

Molecular Pharmacology Fast Forward. Published on August 6, 2020 as DOI: 10.1124/mol.120.119412
This article has not been copyedited and formatted. The final version may differ from this version.

HAL (0.05%) and CAF (50 μM). This increase in P_o resulted from decreasing mean closed time (τ_c) from 19.55 to 1.19 ms and increasing mean open time (τ_o) from 0.56 to 1.86 ms for Level 1 (**Fig 5, Traces A&B**) and was coincident with the appearance of a second channel (Level 2; **Fig 5, Trace C**). At these concentrations, CAF alone had no influence on channel P_o, whereas HAL alone increases P_o by nearly 5-fold (**Fig 6A-C**). However, HAL+CAF in combination increased channel P_o an average of 18-fold over their respective baselines in three separate experiments.

HAL and CAF synergize RYR1-mediated intracellular Ca^{2+} release: To test the hypothesis that synergism between CAF and HAL observed *in vivo* and in single-channel measurements we performed single-cell Ca^{2+} imaging experiments with myotubes cultured from adult HET and WT mice, an established model to investigate MH susceptibility. Despite the fact that HET myotubes had only 40% of the releasable SR Ca^{2+} stores compared to WT, demonstrated by the smaller Ca^{2+} transient amplitude produced by 20 mM CAF (**Fig 7A, B**), HET cells were more sensitive to HAL (0.05% vol/vol) (**Fig 7A, C**). Importantly, the combination of HAL and CAF produced a greatly synergized response in both genotypes compared to either drug alone (**Fig 7A-C**), but the degree of synergism was significantly greater in HET than WT with CAF $\leq$ 0.25 mM due to a left-shift in the concentration-effect curve by up to one order of magnitude (**Fig 7A, C**). Despite the diminished SR Ca^{2+} content in HET myotubes, their sensitivity to HAL+CAF was significantly greater when normalized to the release elicited by 20 mM caffeine, although this distinction converged at higher CAF concentrations $\geq$ 0.5 mM (**Fig 7C**).

Molecular Pharmacology Fast Forward. Published on August 6, 2020 as DOI: 10.1124/mol.120.119412
This article has not been copyedited and formatted. The final version may differ from this version.

Discussion

A seminal finding in the present study identifies a common dietary factor, CAF intake, synergizes adverse outcomes during maintenance anesthesia with a halogenated volatile general anesthetic, exemplified by HAL in our study, in a mouse model (R163C-RYR1; HET) of human MH susceptibility. A second new finding identifies a dominant central influence of CAF and HAL, singly or in combination, that precede the canonical peripheral manifestation of fulminant MH when core body temperature is clamped within the physiological range. The synergistic actions of CAF+HAL exposures in HET mice elicits an ADR *in vivo* at blood CAF concentrations (range of 5-30 μM) well below those needed to trigger SR Ca^{2+} release from WT or HET skeletal myotubes (>100 μM). Measurements of RYR1 channels isolated from WT provide evidence of significant synergism of the modest influence of 0.05% HAL (20 μM), with CAF (50 μM) enhancing RYR1 open probability nearly 30-fold. The synergistic effects of CAF+HAL can be demonstrated in WT and HET myotubes, although it is clear that the synergistic actions are greatly amplified in the HET genotype.

Direct muscle effects alone cannot fully explain our current findings with the combination of CAF and/or HAL *in vivo*. Exposure of HET mice to dietary CAF that produces median plasma concentrations commensurate with those measured in human populations (Barone and Roberts 1996; de Leon et al. 2003; Mitchell et al. 2014; Smith et al. 1982) significantly shortens the time to achieve isoelectric EEG (isoEEG) as well as respiratory and cardiac (ECG) arrest in HET mice. Interestingly, HET mice do not differ from WT in their baseline EEG_{TP} or blood chemistries, regardless of whether they were exposed to dietary CAF. These results suggest that HET mice do not differ in cortical

Molecular Pharmacology Fast Forward. Published on August 6, 2020 as DOI: 10.1124/mol.120.119412
This article has not been copyedited and formatted. The final version may differ from this version.

electrical activity from WT mice during baseline recording under the experimental conditions used in the present study. The lack of differences in baseline EEG_{TP} measured in HET mice during the baseline period, regardless of treatment, also extended to the EEG spectra (data not shown). Although the electrographic study (**Cohort 2**) was powered based on the large effect size observed with of dietary CAF on time to respiratory arrest in HET mice (**Cohort 1**), it should be viewed in light of its pilot design for generating hypotheses regarding the central influences of CAF in synergizing general volatile anesthetics and possible other triggering agents in MHS individuals. Nevertheless, a recently published study of HET mice provided a detailed comparison of whole-body energetics and voluntary activity in HET and WT mice (Rutkowsky et al. 2020). No genotype differences were apparent in voluntary movement measured in a calorimetry chamber or decreased 24-hour energy expenditure, especially during the dark cycle when mice are most active (Rutkowsky et al. 2020). This study provides additional evidence that HET mice in their home cage environment do not differ in arousal, as measured by Baseline EEG_{TP}, compared to WT mice.

Only during maintenance anesthesia with HAL did EEG_{TP} decline in a genotype, CAF treatment and treatment*time dependent manner. Administration of HAL anesthesia to HET mice resulted in the loss of EEG activity before detectable alterations in ECG patterns, regardless of whether the animals received CAF. Under the conditions used that maintain core temperature, blood drawn at the time of death (loss of detectable ECG) indicates only mild to moderate hyperkalemia and acidosis in euthermic HET mice compared to HET mice that are permitted to proceed a fulminant MH episode. Collectively, these data indicate central nervous system mechanisms contribute to

susceptibility of HET mice to lethal consequences of HAL anesthesia, even in the absence of dietary CAF, and that CAF greatly synergizes the effects of this anesthetic. The observation that DAN delays the time to isoEEG, respiratory and cardiac arrest in a time dependent manner further suggesting that the synergistic actions of dietary CAF and HAL in HET mice may be mediated through a common mechanism involving RYRs. This interpretation is supported by results obtained from myotube and single RYR1 channel experiments.

The central effects of dietary CAF are well documented and primarily mediated by its potent antagonism of adenosine receptors, causing increased excitatory neurotransmitter release that lower neuronal activation threshold (Keane et al. 2007; Keane and James 2008; Nehlig et al. 1992; Phillis et al. 1979). Adenosine A2A receptors (A2AR) are found in brain areas rich in dopamine D2 receptors such as the basal ganglia and changes induced by CAF within the basal ganglia would very likely exert a downstream effect on the motor cortex (Ferre et al. 1997; Fisone et al. 2004). However, CAF also antagonizes adenosine A2AR directly within the motor cortex by inhibiting the release of GABA, thus reducing GABAergic inhibitory transmission in the motor cortex (Cerqueira et al. 2006). Expression of Ryr1 mRNA within brain regions, including cortical motor regions, has been documented, although less abundantly than RYR2 (Furuichi et al. 1994; Giannini and Sorrentino 1995; Mori et al. 2000), although data from immunolabeling and western studies for RYR1 protein are more limited (Feng et al. 2017; Hertle and Yeckel 2007), possibly due to antibody cross-reactivity. Behavioral studies using MH susceptible mice arguably provide stronger evidence for a functional role of RYR1 in the mammalian nervous system (Keil et al. 2019; Wayman et al. 2012).

There are a few studies in MH susceptible pigs that suggest alterations in cerebral cortical activity measured by electroencephalograms (EEG) recording during the onset of the fulminant MH crisis in pigs (R615C-RYR1) (Artru and Gronert 1980; Kochs et al. 1990; Kochs E 1990) and horses (R2454G-RYR1) (Aleman et al. 2005). Results from two studies with MH susceptible pigs showed significant depression of EEG activity preceding the onset of cardiovascular and metabolic changes during induction of halothane-triggered fulminant MH (Kochs et al. 1990) (Kochs E 1990). One of these studies documented the temporal decrease in total power concomitant with a shift to lower frequencies (delta-theta activity) in the EEG of MH susceptible pigs maintained with 1% halothane and these alternations preceded the development of fulminant MH (Kochs et al. 1990).

Moreover, altered EEG patterns in MH susceptible pigs were not the result of hypotension, hypoxia, or hypercapnia, leading the authors to speculate that changes in brain wave activity were either due to systemic factors unrelated to the acute MH crisis or involvement of the CNS as a primary target in the pathophysiology of the fulminant MH syndrome (Kochs et al. 1990). In another study, EEG alterations during halothane anesthesia were interpreted as secondary to heat-induced CNS injury resulting from the fulminant MH episode (Forrest et al. 2015), a variable tightly controlled in the present study.

The question arises as to why CAF+HAL act synergistically on RYR1 channels isolated from WT tissue while producing no ADRs in WT mice exposed HAL up to 60 min. EC coupling in skeletal muscle requires precise physical interactions between voltage-gated Ca^{2+} channels ($CaV_{1.1}$) in the T-Tubule and RYR1 residing in the terminal cisternae

Molecular Pharmacology Fast Forward. Published on August 6, 2020 as DOI: 10.1124/mol.120.119412
This article has not been copyedited and formatted. The final version may differ from this version.

of SR (Franzini-Armstrong 2018). Their interactions engage bidirectional signaling, both orthograde activation of RYR1 and retrograde activation of $CaV_{1.1}$ current (Nakai et al. 1996). There is strong evidence for reciprocal negative regulation of the two channels, especially orthograde suppression of RYR1 channel activity by $CaV_{1.1}$, that physiologically dampen both resting Ca^{2+} in the myoplasm by controlling RYR1 mediated Ca^{2+} leak and control Ca^{2+} release properties during EC coupling (Bannister et al. 2009; Eltit et al. 2012; Pessah et al. 1997). MH mutations weaken several aspects of $CaV_{1.1}$-RYR1 negative regulation increasing RYR1 leak responsible for the chronically elevated resting Ca^{2+} observed in the affected myoplasm and depleted SR Ca^{2+} stores (Bannister et al. 2010; Eltit et al. 2012; Esteve et al. 2010; Yang et al. 2006) and explains the inherently high open probabilities of RYR1 channels isolated from R163C-RYR1 (HET mouse used in the present study) and T4826I-RYR1 HET and HOM MH susceptible mouse muscle, which lack $CaV_{1.1}$ and negative regulation (Barrientos et al. 2012; Feng et al. 2011). MH mutations also alter excitation-coupled Ca^{2+} entry mediated by $CaV_{1.1}$ (Bannister et al. 2010; Cherednichenko et al. 2008; Yang et al. 2006). Based on the present findings we posit that triadic complexes that possess RYR1 mutations conferring MH susceptibility are more sensitive to pharmacologic dysregulation by HAL and related triggering anesthetics, and that dietary levels of CAF greatly synergizes these disruptive influences as clearly demonstrated *in vitro* here. These results may provide a mechanistic framework for understanding a recent report that CAF markedly augments neurotoxicity of isoflurane in the fetal macaque brain and may have more general impacts on susceptible life stages (Nogouchi et al. 2018).

Our study provides the first evidence of pharmacological synergism between a general volatile anesthetic and dietary CAF in a mouse model of MH susceptibility. The

study also demonstrates early central nervous system involvement mediating adverse outcomes to dietary CAF during maintenance anesthesia with an exemplary triggering agent HAL. Dietary CAF is a modifiable lifestyle factor that may mitigate risks associated with MH causing mutations in RYR1.

Acknowledgements

We acknowledge the guidance of Professor Alan Buckpitt in establishing the HPLC method for quantifying plasma CAF levels.

Molecular Pharmacology Fast Forward. Published on August 6, 2020 as DOI: 10.1124/mol.120.119412
This article has not been copyedited and formatted. The final version may differ from this version.

Authorship Contributions

Project conception: Pessah

Participated in research design: Pessah, Aleman, Zhang, Lopez, Feng, Cherednichenko

Conducted experiments: Zhang, Aleman, Feng, Cherednichenko, Lopez, Dong

Performed data analysis: Pessah, Feng, Qi, Zhang, Crowe, Cherednichenko Aleman, Lopez

Wrote or contributed to the writing of the manuscript: Pessah, Feng, Zhang, Qi, Crowe, Cherednichenko, Aleman, Lopez

References

Adeokun AM, West SP, Ellis FR, Halsall PJ, Hopkins PM, Foroughmand AM, et al. 1997. The g1021a substitution in the RyR1 gene does not cosegregate with malignant hyperthermia susceptibility in a british pedigree. American journal of human genetics 60:833-841.

Aleman M, Riehl J, Aldridge BM, Lecouteur RA, Stott JL, Pessah IN. 2004. Association of a mutation in the ryanodine receptor 1 gene with equine malignant hyperthermia. Muscle Nerve 30:356-365.

Aleman M, Brosnan RJ, Williams DC, LeCouteur RA, Imai A, Tharp BR, et al. 2005. Malignant hyperthermia in a horse anesthetized with halothane. Journal of veterinary internal medicine / American College of Veterinary Internal Medicine 19:363-366.

Artru AA, Gronert GA. 1980. Cerebral metabolism during porcine malignant hyperthermia. Anesthesiology 53:121-126.

Bannister RA, Pessah IN, Beam KG. 2009. The skeletal l-type ca(2+) current is a major contributor to excitation-coupled ca(2+) entry. The Journal of general physiology 133:79-91.

Bannister RA, Esteve E, Eltit JM, Pessah IN, Allen PD, Lopez JR, et al. 2010. A malignant hyperthermia-inducing mutation in RyR1 (R163C): Consequent alterations in the functional properties of dhpr channels. The Journal of general physiology 135:629-640.

Barone JJ, Roberts HR. 1996. Caffeine consumption. Food Chem Toxicol 34:119-129.

Barrientos GC, Feng W, Truong K, Matthaei KI, Yang T, Allen PD, et al. 2012. Gene dose influences cellular and calcium channel dysregulation in heterozygous and homozygous T4826I-RyR1 malignant hyperthermia-susceptible muscle. J Biol Chem 287:2863-2876.

Beam KG, Knudson CM. 1988. Calcium currents in embryonic and neonatal mammalian skeletal muscle. J Gen Physiol 91:781-798.

Benjamini Y, Hochberg Y. (1995). Controlling the False Discovery Rate: A Practical and Powerful Approach to Multiple Testing. *J Royal Statis Soc, B*, 57, 289–300.

Brandom BW, Bina S, Wong CA, Wallace T, Visoiu M, Isackson PJ, et al. 2013. Ryanodine receptor type 1 gene variants in the malignant hyperthermia-susceptible population of the united states. Anesth Analg 116:1078-1086.

Brooks SP, Storey KB. 1992. Bound and determined: A computer program for making buffers of defined ion concentrations. Anal Biochem 201:119-126.

Cerqueira V, de Mendonca A, Minez A, Dias AR, de Carvalho M. 2006. Does caffeine modify corticomotor excitability? Neurophysiol Clin 36:219-226.

Chelu MG, Goonasekera SA, Durham WJ, Tang W, Lueck JD, Riehl J, et al. 2006. Heat- and anesthesia-induced malignant hyperthermia in an RyR1 knock-in mouse. FASEB journal : official publication of the Federation of American Societies for Experimental Biology 20:329-330.

Cherednichenko G, Ward CW, Feng W, Cabrales E, Michaelson L, Samso M, et al. 2008. Enhanced excitation-coupled calcium entry in myotubes expressing malignant hyperthermia mutation R163C is attenuated by dantrolene. Molecular pharmacology 73:1203-1212.

Cornelis MC, El-Sohemy A, Kabagambe EK, Campos H. 2006. Coffee, cyp1a2 genotype, and risk of myocardial infarction. JAMA 295:1135-1141.

de Leon J, Diaz FJ, Rogers T, Browne D, Dinsmore L, Ghosheh OH, et al. 2003. A pilot study of plasma caffeine concentrations in a us sample of smoker and nonsmoker volunteers. Prog Neuropsychopharmacol Biol Psychiatry 27:165-171.

Ding M, Bhupathiraju SN, Satija A, van Dam RM, Hu FB. 2014. Long-term coffee consumption and risk of cardiovascular disease: A systematic review and a dose-response meta-analysis of prospective cohort studies. Circulation 129:643-659.

Eltit JM, Bannister RA, Moua O, Altamirano F, Hopkins PM, Pessah IN, et al. 2012. Malignant hyperthermia susceptibility arising from altered resting coupling between the skeletal muscle l-type ca2+ channel and the type 1 ryanodine receptor. Proceedings of the National Academy of Sciences of the United States of America 109:7923-7928.

Esteve E, Eltit JM, Bannister RA, Liu K, Pessah IN, Beam KG, et al. 2010. A malignant hyperthermia-inducing mutation in RyR1 (R163C): Alterations in ca2+ entry, release, and retrograde signaling to the dhpr. The Journal of general physiology 135:619-628.

Feng W, Barrientos GC, Cherednichenko G, Yang T, Padilla IT, Truong K, et al. 2011. Functional and biochemical properties of ryanodine receptor type 1 channels from heterozygous R163C malignant hyperthermia-susceptible mice. Molecular pharmacology 79:420-431.

Feng W, Zheng J, Robin G, Dong Y, Ichikawa M, Inoue Y, et al. 2017. Enantioselectivity of 2,2',3,5',6-pentachlorobiphenyl (pcb 95) atropisomers toward ryanodine receptors (RyRs) and their influences on hippocampal neuronal networks. Environ Sci Technol 51:14406-14416.

Ferre S, Fredholm BB, Morelli M, Popoli P, Fuxe K. 1997. Adenosine-dopamine receptor-receptor interactions as an integrative mechanism in the basal ganglia. Trends Neurosci 20:482-487.

Findley AS, Richards AL, Petrini C, Alazizi A, Doman E, Shanku AG, et al. 2019. Interpreting coronary artery disease risk through gene-environment interactions in gene regulation. Genetics 213:651-663.

Fisone G, Borgkvist A, Usiello A. 2004. Caffeine as a psychomotor stimulant: Mechanism of action. Cell Mol Life Sci 61:857-872.

Fitzmaurice GM, Laird NM, Ware JH. 2004. Applied Longitudinal Analysis. John Wiley & Sons. pp. 326–328.

Forrest KM, Foulds N, Millar JS, Sutherland PD, Pappachan VJ, Holden S, et al. 2015. RyR1-related malignant hyperthermia with marked cerebellar involvement - a paradigm of heat-induced cns injury? Neuromuscul Disord 25:138-140.

Franzini-Armstrong C. 2018. The relationship between form and function throughout the history of excitation-contraction coupling. J Gen Physiol 150:189-210.

Fujii J, Otsu K, Zorzato F, de Leon S, Khanna VK, Weiler JE, et al. 1991. Identification of a mutation in porcine ryanodine receptor associated with malignant hyperthermia. Science 253:448-451.

Furuichi T, Furutama D, Hakamata Y, Nakai J, Takeshima H, Mikoshiba K. 1994. Multiple types of ryanodine receptor/ca2+ release channels are differentially expressed in rabbit brain. J Neurosci 14:4794-4805.

Giannini G, Sorrentino V. 1995. Molecular structure and tissue distribution of ryanodine receptors calcium channels. Med Res Rev 15:313-323.

Gillies RL, Bjorksten AR, Davis M, Du Sart D. 2008. Identification of genetic mutations in australian malignant hyperthermia families using sequencing of RyR1 hotspots. Anaesth Intensive Care 36:391-403.

Gillies RL, Bjorksten AR, Du Sart D, Hockey BM. 2015. Analysis of the entire ryanodine receptor type 1 and alpha 1 subunit of the dihydropyridine receptor (cacna1s) coding regions for variants associated with malignant hyperthermia in australian families. Anaesth Intensive Care 43:157-166.

Giulivi C, Ross-Inta C, Omanska-Klusek A, Napoli E, Sakaguchi D, Barrientos G, et al. 2011. Basal bioenergetic abnormalities in skeletal muscle from ryanodine receptor malignant hyperthermia-susceptible R163C knock-in mice. The Journal of biological chemistry 286:99-113.

Hartmann M, Czok G. 1980. [pharmacokinetics of caffeine in mice and its modification by ethanol]. Z Ernahrungswiss 19:215-227.

Hertle DN, Yeckel MF. 2007. Distribution of inositol-1,4,5-trisphosphate receptor isotypes and ryanodine receptor isotypes during maturation of the rat hippocampus. Neuroscience 150:625-638.

Hopkins PM, Ruffert H, Snoeck MM, Girard T, Glahn KP, Ellis FR, et al. 2015. European malignant hyperthermia group guidelines for investigation of malignant hyperthermia susceptibility. Br J Anaesth 115:531-539.

Ibarra Moreno CA, Hu S, Kraeva N, Schuster F, Johannsen S, Rueffert H, et al. 2019. An assessment of penetrance and clinical expression of malignant hyperthermia in individuals carrying diagnostic ryanodine receptor 1 gene mutations. Anesthesiology.

Jungbluth H, Treves S, Zorzato F, Sarkozy A, Ochala J, Sewry C, et al. 2018. Congenital myopathies: Disorders of excitation-contraction coupling and muscle contraction. Nat Rev Neurol 14:151-167.

Keane MA, James JE, Hogan MJ. 2007. Effects of dietary caffeine on topographic eeg after controlling for withdrawal and withdrawal reversal. Neuropsychobiology 56:197-207.

Keane MA, James JE. 2008. Effects of dietary caffeine on eeg, performance and mood when rested and sleep restricted. Hum Psychopharmacol 23:669-680.

Keil KP, Sethi S, Wilson MD, Silverman JL, Pessah IN, Lein PJ. 2019. Genetic mutations in ca(2+) signaling alter dendrite morphology and social approach in juvenile mice. Genes Brain Behav 18:e12526.

Kleiber M. 1947. Body size and metabolic rate. Physiol Rev 27:511-541.

Klem GH, Luders HO, Jasper HH, Elger C. 1999. The ten-twenty electrode system of the international federation. The international federation of clinical neurophysiology. Electroencephalogr Clin Neurophysiol Suppl 52:3-6.

Kochs E, Hoffman WE, Roewer N, Schulte am Esch J. 1990. Alterations in brain electrical activity may indicate the onset of malignant hyperthermia in swine. Anesthesiology 73:1236-1242.

Kochs E, Hoffman WE, Schulte am Esch J. 1993. Improvement of brain electrical activity during treatment of porcine malignant hyperthermia with dantrolene. Br J Anaesth 71:881-884.

Kochs E NH, Schulte am Esch J. 1990. Characteristics of cerebra blood flow and the electroencephalogram during experimental malignant hyperthermia. Anasth Intensivther Notfallmed 25:348-353.

Korekar G, Kumar A, Ugale C. 2019. Occurrence, fate, persistence and remediation of caffeine: a review. *Environ Sci Pollut Res Int*. Dec 07 doi:10.1007/s11356-019-06998-8.

Kramer, CY (1956). “Extension of Multiple Range Tests to Group Means with Unequal Numbers of Replications.” Biometrics 12:307–310.

Laird, NM, Ware JH. (1982). Random-Effects Models for Longitudinal Data. Biometrics. International Biometric Society. ***38*** *(4): 963-974*

Litman RS, Griggs SM, Dowling JJ, Riazi S. 2018. Malignant hyperthermia susceptibility and related diseases. Anesthesiology 128:159-167.

Lopez JR, Kaura V, Diggle CP, Hopkins PM, Allen PD. 2018. Malignant hyperthermia, environmental heat stress, and intracellular calcium dysregulation in a mouse model expressing the p.G2435r variant of RyR1. Br J Anaesth 121:953-961.

McCarthy TV, Healy JM, Heffron JJ, Lehane M, Deufel T, Lehmann-Horn F, et al. 1990. Localization of the malignant hyperthermia susceptibility locus to human chromosome 19q12-13.2. Nature 343:562-564.

Miller DM, Daly C, Aboelsaod EM, Gardner L, Hobson SJ, Riasat K, et al. 2018. Genetic epidemiology of malignant hyperthermia in the uk. Br J Anaesth 121:944-952.

Mitchell DC, Knight CA, Hockenberry J, Teplansky R, Hartman TJ. 2014. Beverage caffeine intakes in the u.S. Food Chem Toxicol 63:136-142.

Mori F, Fukaya M, Abe H, Wakabayashi K, Watanabe M. 2000. Developmental changes in expression of the three ryanodine receptor mrnas in the mouse brain. Neurosci Lett 285:57-60.

Nakai J, Dirksen RT, Nguyen HT, Pessah IN, Beam KG, Allen PD. 1996. Enhanced dihydropyridine receptor channel activity in the presence of ryanodine receptor. Nature 380:72-75.

Nehlig A, Daval JL, Debry G. 1992. Caffeine and the central nervous system: Mechanisms of action, biochemical, metabolic and psychostimulant effects. Brain Res Brain Res Rev 17:139-170.

Palatini P, Ceolotto G, Ragazzo F, Dorigatti F, Saladini F, Papparella I, et al. 2009. Cyp1a2 genotype modifies the association between coffee intake and the risk of hypertension. J Hypertens 27:1594-1601.

Pessah IN, Molinski TF, Meloy TD, Wong P, Buck ED, Allen PD, et al. 1997. Bastadins relate ryanodine-sensitive and -insensitive ca2+ efflux pathways in skeletal sr and bc3h1 cells. The American journal of physiology 272:C601-614.

Phillis JW, Edstrom JP, Kostopoulos GK, Kirkpatrick JR. 1979. Effects of adenosine and adenine nucleotides on synaptic transmission in the cerebral cortex. Can J Physiol Pharmacol 57:1289-1312.

Rando TA, Blau HM. 1994. Primary mouse myoblast purification, characterization, and transplantation for cell-mediated gene therapy. J Cell Biol 125:1275-1287.

Ratto D, Joyner RW. 2019. Dantrolene. In: Statpearls. Treasure Island (FL).

Roberts MC, Mickelson JR, Patterson EE, Nelson TE, Armstrong PJ, Brunson DB, et al. 2001. Autosomal dominant canine malignant hyperthermia is caused by a mutation in the gene encoding the skeletal muscle calcium release channel (RyR1). Anesthesiology 95:716-725.

Robinson RL, Anetseder MJ, Brancadoro V, van Broekhoven C, Carsana A, Censier K, et al. 2003. Recent advances in the diagnosis of malignant hyperthermia susceptibility: How confident can we be of genetic testing? Eur J Hum Genet 11:342-348.

Rosen GP, Escobar M, Fumero P, Viswanath O, Wright J. 2019. The importance of a prepared and ready malignant hyperthermia response team. J Clin Anesth 56:109-110.

Rosenberg H, Pollock N, Schiemann A, Bulger T, Stowell K. 2015. Malignant hyperthermia: A review. Orphanet J Rare Dis 10:93.

Rutkowsky JM, Knotts TA, Allen PD, Pessah IN, Ramsey JJ. 2020. Sex-specific alterations in whole body energetics and voluntary activity in heterozygous R163C malignant hyperthermia-susceptible mice [published online ahead of print, 2020 May 4. *FASEB J*. 2020;10.1096/fj.202000403. https://doi:10.1096/fj.202000403.

Smith JM, Pearson S, Marks V. 1982. Plasma caffeine concentration in outpatients. Lancet 2:985-986.

Truong KM, Pessah IN. 2019. Comparison of chlorantraniliprole and flubendiamide activity toward wild-type and malignant hyperthermia-susceptible ryanodine receptors and heat stress intolerance. Toxicol Sci 167:509-523.

Voermans NC, Snoeck M, Jungbluth H. 2016. RyR1-related rhabdomyolysis: A common but probably underdiagnosed manifestation of skeletal muscle ryanodine receptor dysfunction. Rev Neurol (Paris) 172:546-558.

Wayman GA, Yang D, Bose DD, Lesiak A, Ledoux V, Bruun D, et al. 2012. Pcb-95 promotes dendritic growth via ryanodine receptor-dependent mechanisms. Environmental health perspectives 120:997-1002.

Williams DC, Aleman M, Holliday TA, Fletcher DJ, Tharp B, Kass PH, et al. 2008. Qualitative and quantitative characteristics of the electroencephalogram in normal horses during spontaneous drowsiness and sleep. J Vet Intern Med 22:630-638.

Yang A, Palmer AA, de Wit H. 2010. Genetics of caffeine consumption and responses to caffeine. Psychopharmacology (Berl) 211:245-257.

Yang T, Riehl J, Esteve E, Matthaei KI, Goth S, Allen PD, et al. 2006. Pharmacologic and functional characterization of malignant hyperthermia in the R163C RyR1 knock-in mouse. Anesthesiology 105:1164-1175.

Yuen B, Boncompagni S, Feng W, Yang T, Lopez JR, Matthaei KI, et al. 2012. Mice expressing T4826I-RyR1 are viable but exhibit sex- and genotype-dependent susceptibility to malignant hyperthermia and muscle damage. FASEB journal : official publication of the Federation of American Societies for Experimental Biology 26:1311-1322.

Zhou A, Hypponen E. 2019. Long-term coffee consumption, caffeine metabolism genetics, and risk of cardiovascular disease: A prospective analysis of up to 347,077 individuals and 8368 cases. Am J Clin Nutr 109:509-516.

Zhou J, Bose D., Allen, P. D., and Pessah, I. N. . 2014. Malignant hyperthermia and other related disorders. Philadelphia, PA:Elsevier Health Sciences, NY, NY.

Molecular Pharmacology Fast Forward. Published on August 6, 2020 as DOI: 10.1124/mol.120.119412
This article has not been copyedited and formatted. The final version may differ from this version.

Footnotes

*Funding: This work was supported by National Institutes of Environmental Health Sciences grant [ES R014901] and [P42 ES004699], The National Science Foundation [1840842] and The National Institute of Arthritis and Musculoskeletal Sciences [P01 AR052354]. The research was also supported by the UC Davis Equine and Comparative Neurology Research Group (MA).

§Present address: Department of Research, Mount Sinai Medical Center, Miami, FL 33140, USA

†Contributed equally

@Correspondence: Dr. Isaac N. Pessah, Molecular Biosciences, School of Veterinary Medicine, University of California, Davis, CA 95616 USA email: inpessah@ucdavis.edu; Phone: 530-752-6696

Dr. Monica Aleman, Departments of Medicine and Epidemiology, School of Veterinary Medicine, University of California, Davis CA 95616, email: mraleman@ucdavis.edu Phone: 530-752-1363,

Figure Legends

Figure 1. Plasma caffeine (CAF) concentrations from dosed mice detected using HPLC. Mice were provided CAF (0.2 mg/mL) *ad libitum* in drinking water containing 5% sucrose, or VEH containing just 5% sucrose, for ≥7 days. Blood was collected at the conclusion of each experiment. All plasma samples (standards and unknowns) were spiked with an equal concentration of the internal standard benzotriazole (Bza) prior to extraction. **(*A*)** Representative HPLC chromatogram showing the absorbance peaks corresponding to caffeine and benzotriazole at λ = 273 nm. **(*B*)** Representative standard curve correlating known caffeine concentration (spiked blank plasma samples) to the AUC of the detected caffeine peak (AUC_{Caff}) normalized to that of the internal standard (AUC_{Bza}). **(*C*)** Plasma caffeine concentrations determined using this method from both VEH- and CAF-treated (Trough, Peak) mice. Trough values were obtained using blood collected during daytime at the conclusion of *in vivo* experiments; Peak values were obtained from blood collected immediately after euthanasia at nighttime. Box and whiskers represent first quartile, median, third quartile, and range of concentrations detected.

Molecular Pharmacology Fast Forward. Published on August 6, 2020 as DOI: 10.1124/mol.120.119412
This article has not been copyedited and formatted. The final version may differ from this version.

Figure 2. CAF treatment decreases time to respiratory arrest in R163C (HET) mice exposed to halothane (HAL), an effect partially rescued by dantrolene (DAN). WT and HET mice dosed ≥7 d with VEH or CAF to obtain blood levels shown in Figure 1. Mice (Cohort 1) were randomly assigned to one of eight treatment groups as follows: WT+VEH (n=13), WT+CAF (n=16), HET+VEH (n=13), HET+CAF (n=14), HET+VEH+DAN (n=11), HET+CAF+DAN (n=10). Mice were exposed to 1.5% HAL (vol/vol in air). The survival functions (respiratory arrest) were summarized in the Kaplan-Meier survival functions for all six genotype and treatment groups up to 45 min. One set of HET mice received a single dose of DAN (2.5 mg/kg i.p.) before commencing HAL anesthesia (HET+VEH+DAN and HET+CAF+DAN). Survival curves were compared using log-rank/Mantel-Cox test (table insert).

Molecular Pharmacology Fast Forward. Published on August 6, 2020 as DOI: 10.1124/mol.120.119412
This article has not been copyedited and formatted. The final version may differ from this version.

Figure 3. HET mice maintained with 1.5% HAL anesthesia achieve respiratory and cardiac arrests despite maintenance of euthermic core body temperature: Dietary CAF significantly shortens time to adverse drug response, whereas DAN negates effects of CAF. Simultaneous recording of core body temperature (Fig.3A), respiratory (Fig.3B) and ECG (Fig.3C) rates during maintained 1.5% HAL anesthesia for a duration of 40 min were performed as described in Methods. Each genotype and respective treatment group had N=3-4 mice. OriginLab 9.0 was used to perform unpaired *t*-test, and the *p* value, if <0.05 (in red), is regarded as significantly different.

Molecular Pharmacology Fast Forward. Published on August 6, 2020 as DOI: 10.1124/mol.120.119412
This article has not been copyedited and formatted. The final version may differ from this version.

Figure 4. HET mice exposed to dietary CAF shortens time to isoEEG, an effect mitigated by acute DAN intervention. EEG total power (EEG_{TP}) was recorded during the Maintenance period under 1.5% HAL anesthesia. EEG records were binned in 5-min intervals for a total of 50 min. EEG_{TP} during the Maintenance period was normalized to the mean EEG_{TP} taken from each mouse by obtained from 9-12 epochs during the 2 minutes of recording during the Baseline period as described in the Methods. The number of mice in each treatment group was n=3-4 (**Cohort 2**). **Panel A** (WT) and **Panel B** (HET) treatment groups. Statistical analysis for the HET defined for each treatment was conducted with mixed effects models and SAS 9.4 Proc Mixed (SAS Institute, Cary, NC). An adjusted P value < 0.05 was considered statistically significant.

Molecular Pharmacology Fast Forward. Published on August 6, 2020 as DOI: 10.1124/mol.120.119412
This article has not been copyedited and formatted. The final version may differ from this version.

Figure 5. Combination of CAF (50 μM) and HAL (0.05%) synergistically enhance WT RYR1 channel gating activity. (*A*) Exemplary gating activity of WT RYR1 channels when measured in the presence of 2 and 100 μM cytoplasmic (*cis*) and luminal (*trans*) free Ca^{2+} side of the bilayer chamber before and after exposure to the combination of 0.05% (vol/vol in buffer) halothane (HAL) and 50 μM caffeine (CAF). Cs^{+} is the current carrier (see Methods). Panel **A** shows a representative trace of an entire recording. Panels **B** and **C** are expanded 7 sec segments taken from trace **A** indicated by the dashed lines showing finer details of channel gating behavior before and after addition of HAL & CAF. Horizonal arrows and corresponding dashed lines to the right of traces **B** and **C** indicate current amplitude of the channels in the closed state (Level 0), one channel in full conductance (Level 1), and a second channel in full conductance (Level 2). Panel ***D*** summarizes the gating kinetic parameters, mean dwelling time (τ, ms) and opening probability (P_o) of each of the gating level (0, 1 and 2). Representative of n=3 independent channels fusions.

Molecular Pharmacology Fast Forward. Published on August 6, 2020 as DOI: 10.1124/mol.120.119412
This article has not been copyedited and formatted. The final version may differ from this version.

Figure 6. Influence of 50 μM CAF, 0.05% HAL or CAF+HAL on RYR1 single channel gating activity. Cs^+ currents were measured in the presence of 2 μM free Ca^{2+} in *cis* and 100 μM *trans*. The gating of a RYR1 channel was recorded for 1 minute before being exposed to 50 μM CAF (Panel **A**); representative channel from n=3 experiments. Panel **B** shows a representative response to addition of 0.05% HAL (n=2 experiments). The gating parameters of the channel, P_o and the mean dwelling time at closed – Level 0 (τ_0) and open state – Level 1 (τ_1) are denoted by the horizontal arrows to the right of each current trace. Panel **C** summarizes of RYR1 channel open probability for Level 1 (P_o) before and after addition of 50 μM CAF, 0.05% HAL or their combination (HAL+CAF). P_o values were acquired from 10 epochs, 3 sec/bin of each BLM measurement before and after the addition of test compound(s), allowing 20-30 sec of mixing using a micro-magnet stirring device. Panel **C** shows P_o values (Mean ± SD) from RYR1 channels gating at Level 1 before (Control) and after exposed to HAL (n=2), CAF (n=3), or HAL+CAF mixture (n=3). Statistical analysis of unpaired *t*-test was made with software GraphPad (Prism, San Diego, CA USA). Significant difference marked as asterisk *, indicating $p<0.05$.

Molecular Pharmacology Fast Forward. Published on August 6, 2020 as DOI: 10.1124/mol.120.119412
This article has not been copyedited and formatted. The final version may differ from this version.

Figure 7. Synergism between CAF and HAL enhances SR Ca^{2+} release in WT and HET skeletal myotubes. Panel **A**, Representative traces showing cytoplasmic Ca^{2+} responses recorded from WT and HET myotubes loaded with Fluo-4 exposed to the combinations CAF and HAL as indicated. Both genotypes were first exposed to a brief perfusion of CAF 20 mM to assess the filling state of the SR store followed by a washout. Once cytoplasmic Ca^{2+} concentration recovered to original baseline (not shown), myotubes were exposed to a brief perfusion of HAL (0.05% vol/vol in buffer) and allow to recover. Subsequent exposure by perfusion with 0.025-0.5 mM CAF in the presence of HAL (kept constant at 0.05% throughout) were sequentially texted with intervening washout to recover baseline (not shown). Panel **B**, Concentration-effect response relationship of WT (n = 12-13) and HET (n = 8-9) myotubes to brief exposure to CAF alone (0.25-20 mM), indicating that HET myotubes have chronically depleted CAF-sensitive SR Ca^{2+} stores compared to WT. Panel **C**, Data summarizing responses of WT (n = 14) and HET(n = 14) myotubes to low concentrations of CAF (0 - 0.5 mM) in the absence or presence of constant HAL (0.05% vol/vol). Ca^{2+} transient amplitude is expressed as a percent of maximal response elicited by 20 mM CAF. CAF alone had no effect up to 0.5 mM. All data represent mean ± SE. *$p \leq 0.05$, comparing between genotypes at each CAF concentration (One-way ANOVA with Bonferroni's post-test, using OriginLab 9.0).

Molecular Pharmacology Fast Forward. Published on August 6, 2020 as DOI: 10.1124/mol.120.119412
This article has not been copyedited and formatted. The final version may differ from this version.

TABLE 1. HET mice exhibit significantly shorter times to isoEEG. WT and HET mice maintained with 1.5% HAL anesthesia were instrumented to continuously record EEG and ECG as described in the Methods. Data across genotype and treatment condition were analyzed using paired *t*-test (OriginLab 9.0). Each genotype and treatment group had an n=3-4 mice.

Genotype	CAF	DAN	Iso. EEG (Mean±SD) min	ECG Arrest (Mean±SD) min	EEG vs ECG Arrest (*p* value)
WT	-	-	>60.0	>60.0	N/A
	+	-	>60.0	>60.0	N/A
HET	-	-	12.3 ± 1.9	24.2 ± 5.2	0.018
	+	-	8.9 ± 0.8	17.2 ± 4.8	0.036
	+	+	25.8 ± 8.8	32.5 ± 11.7	0.041
	-	+	29.5 ± 9.7	38.5 ± 5.7	0.042

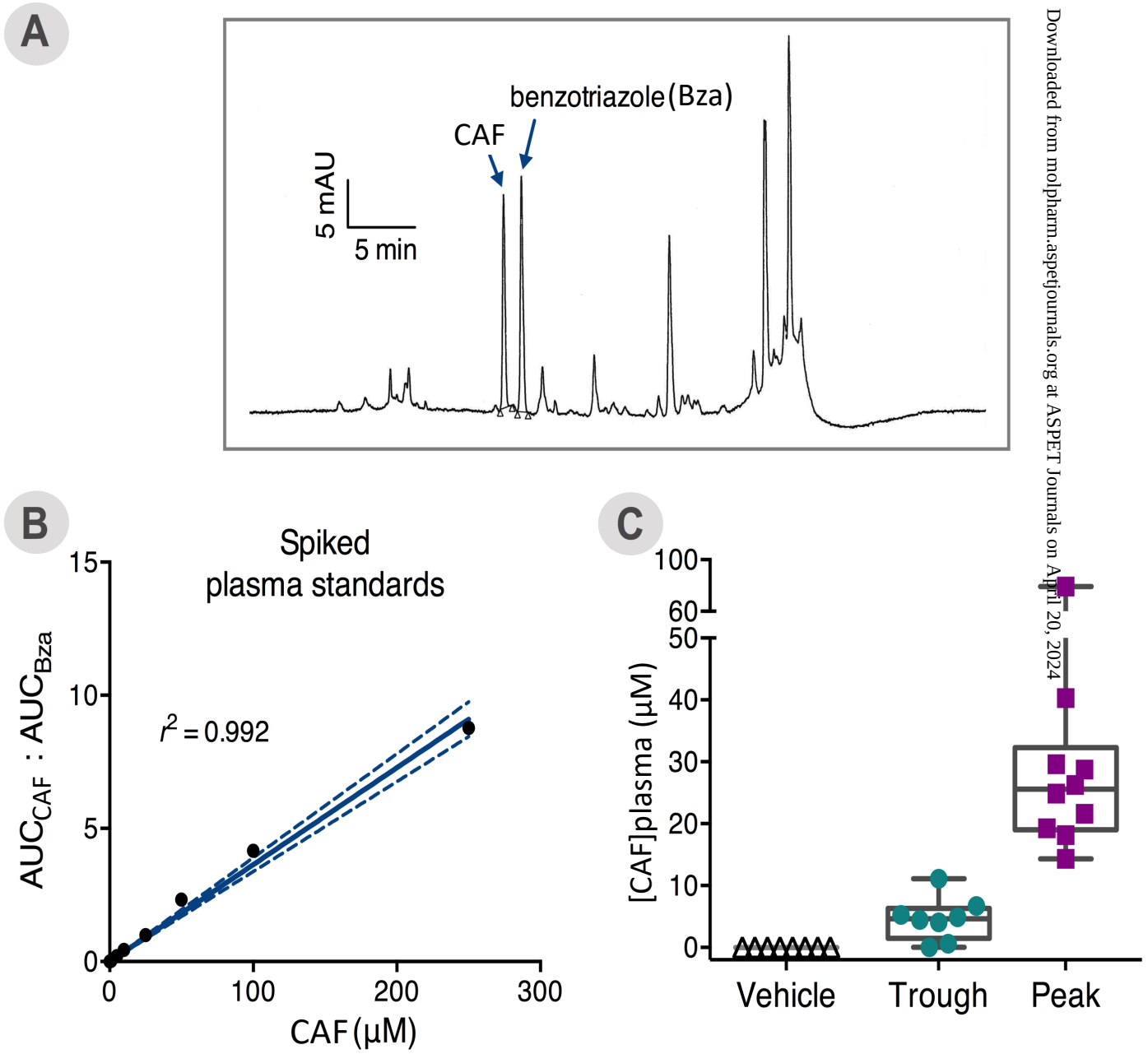

Figure 1

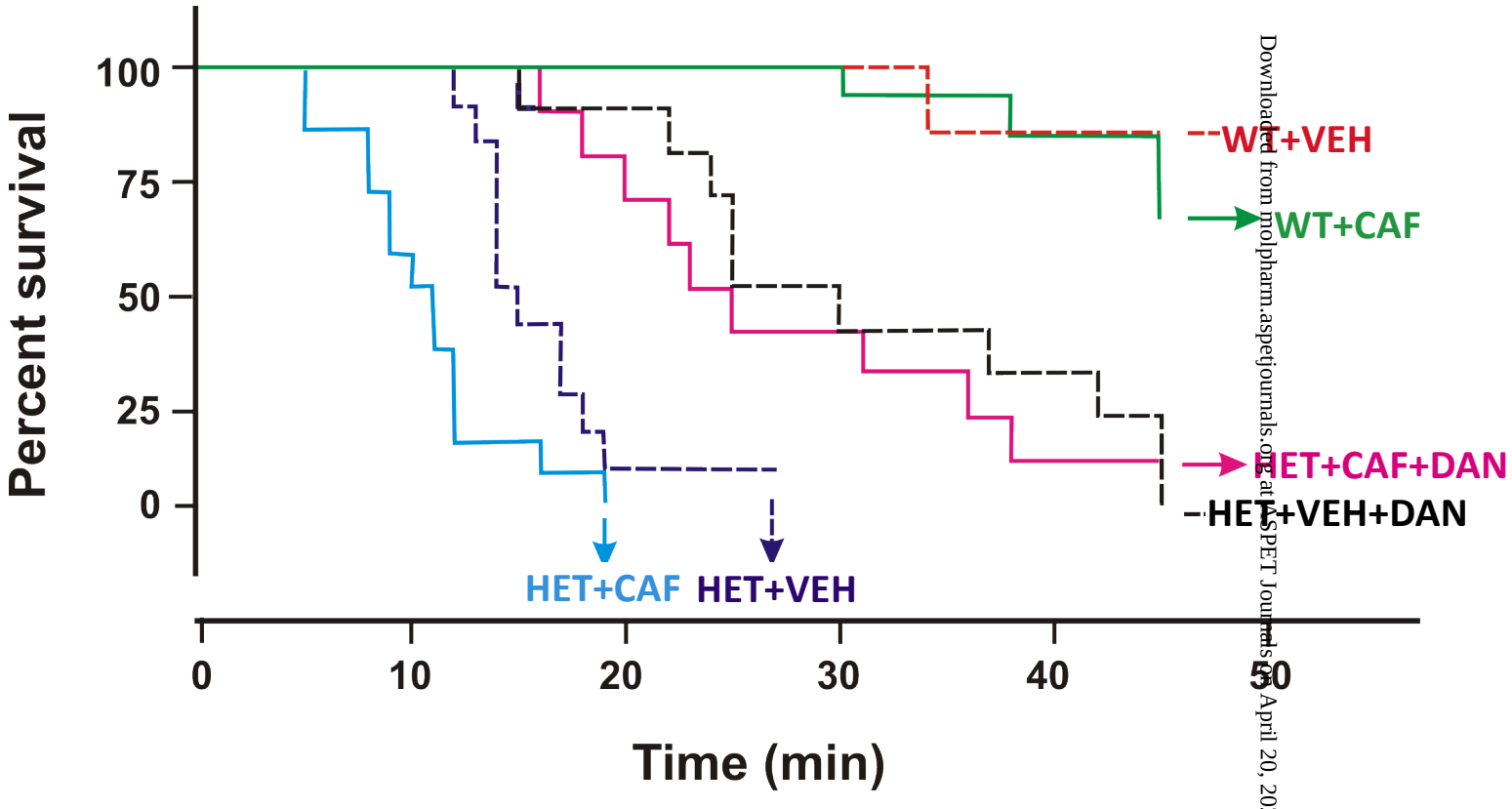

Mantel-Cox

HET	
(HET+VEH) vs (HET+CAF)	*p = 0.0026*
(HET+VEH-DAN) vs (HET+VEH+DAN)	*p = 0.0007*
(HET+CAF) vs (HET+CAF+DAN)	*p < 0.0001*
(HET+VEH+DAN) vs (HET+CAF+DAN)	*p = 0.3820*

Figure 2

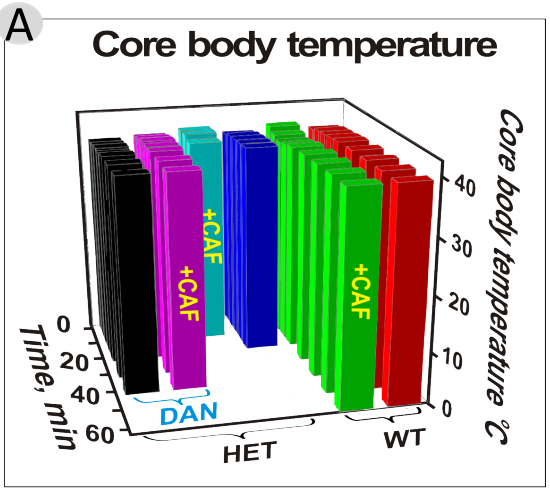

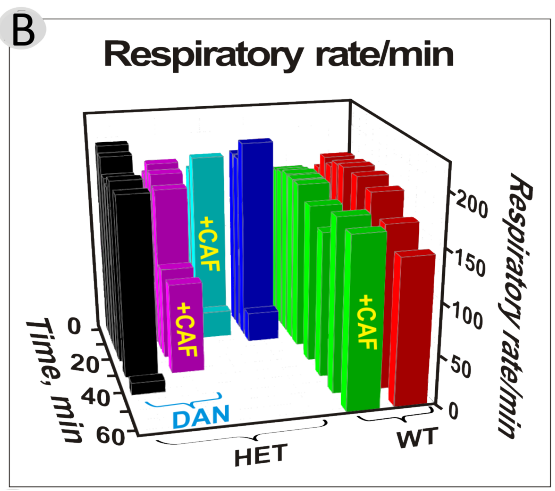

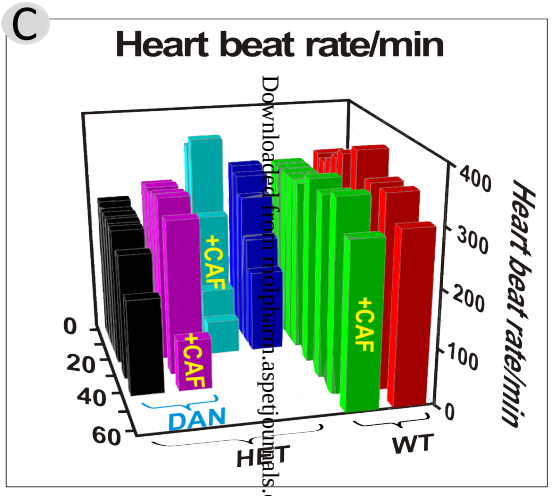

Time to Respitory Arrest, min

Genotype	CAF	DAN	Resp. Arrest (Mean±SD) min
WT	-	-	>60.0
	+	-	>60.0
HET	-	-	14.4 ± 0.8
	+	-	10.2 ± 1.0
	+	+	27.6 ± 8.5
	-	+	33.6 ± 9.9

Genotype-Treatment	*p value*
HET+VEH *vs* HET+CAF	0.005
HET+VEH *vs* HET+CAF+DAN	0.046
HET+VEH *vs* HET+DAN	0.029
HET+CAF *vs* HET+CAF+DAN	0.018
HET+CAF *vs* HET+DAN	0.016
HET+CAF+DAN *vs* HET+DAN	0.426

Time to ECG Arrest, min

Genotype	CAF	DAN	ECG Arrest (Mean±SD) min
WT	-	-	>60.0
	+	-	>60.0
HET	-	-	24.2 ± 5.2
	+	-	17.2 ± 4.8
	+	+	32.5 ± 11.7
	-	+	38.5 ± 5.7

Genotype-Treatment	*p value*
HET+VEH *vs* HET+CAF	0.164
HET+VEH *vs* HET+CAF+DAN	0.310
HET+VEH *vs* HET+DAN	0.032
HET+CAF *vs* HET+CAF+DAN	0.091
HET+CAF *vs* HET+DAN	0.008
HET+CAF+DAN *vs* HET+DAN	0.455

Figure 3

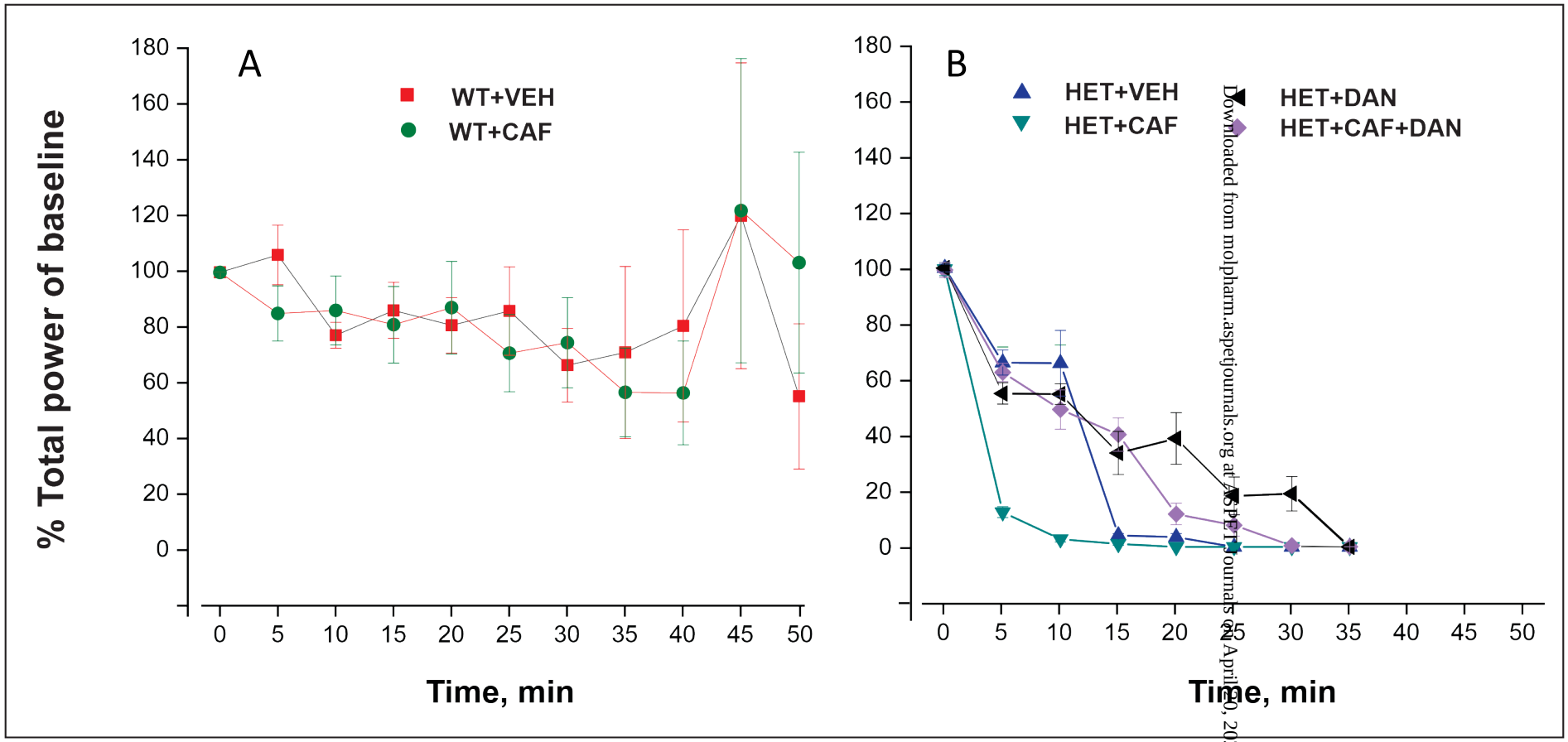

Treatment	Treatment	Raw P (Pr > | t |)	Adjustment	Adj P
HET+VEH	HET+CAF+DAN	0.42	Tukey-Kramer	0.85
HET+VEH	HET+DAN	0.06	Tukey-Kramer	0.25
HET+VEH	HET+CAF	0.005	Tukey-Kramer	0.025
HET+CAF+DAN	HET+DAN	0.24	Tukey-Kramer	0.64
HET+CAF+DAN	HET+CAF	0.0001	Tukey-Kramer	0.0008
HET+DAN	HET+CAF	<0.0001	Tukey-Kramer	<0.0001

Figure 4

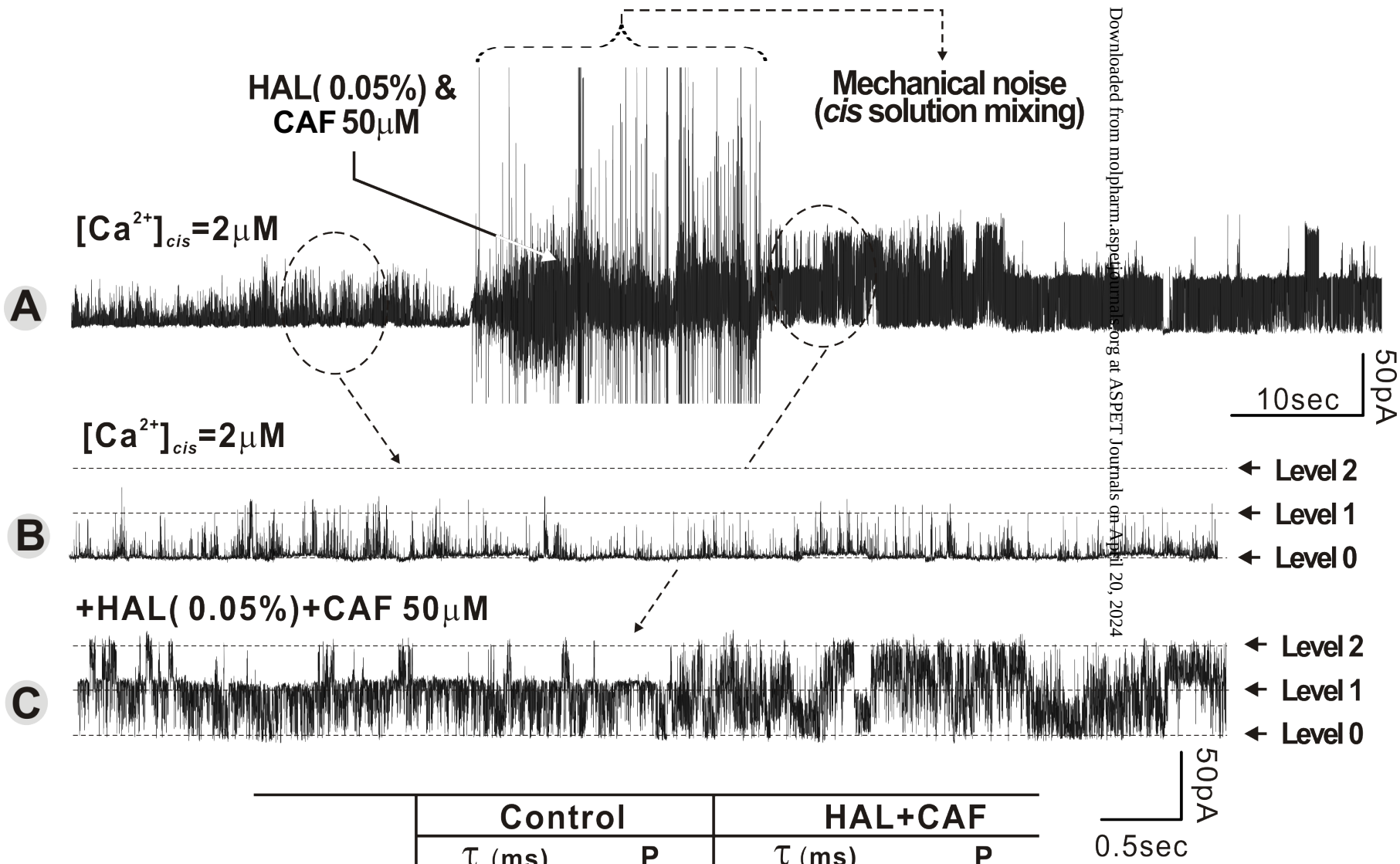

D

	Control		HAL+CAF	
	τ (ms)	P_o	τ (ms)	P_o
Level 0	19.55 ±33.581	N/A	1.19 ± 6.91	N/A
Level 1	0.56 ± 0.49	0.028	1.86 ± 3.10	0.615
Level 2	0	0	1.08 ± 1.24	0.095

Figure 5

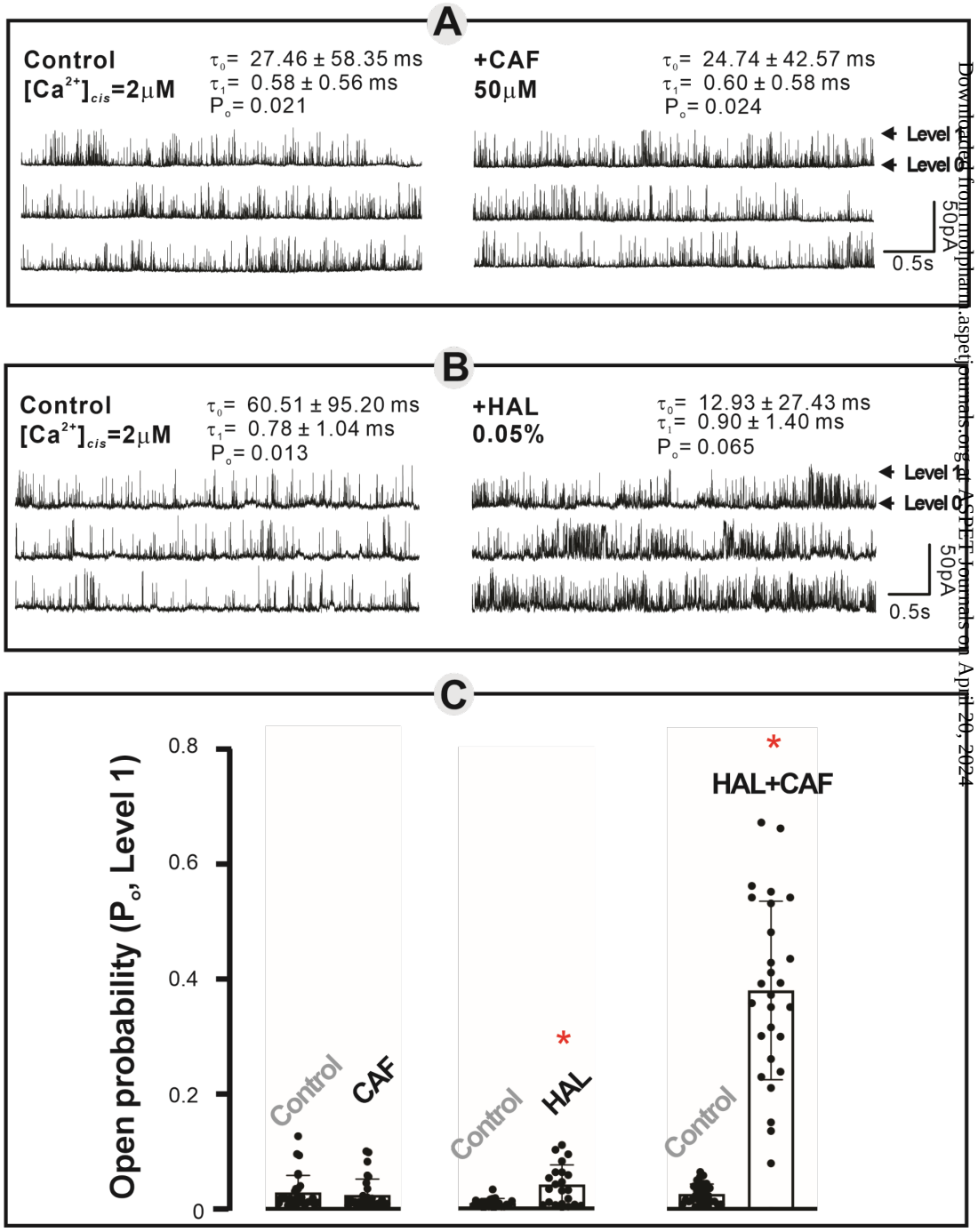

Figure 6

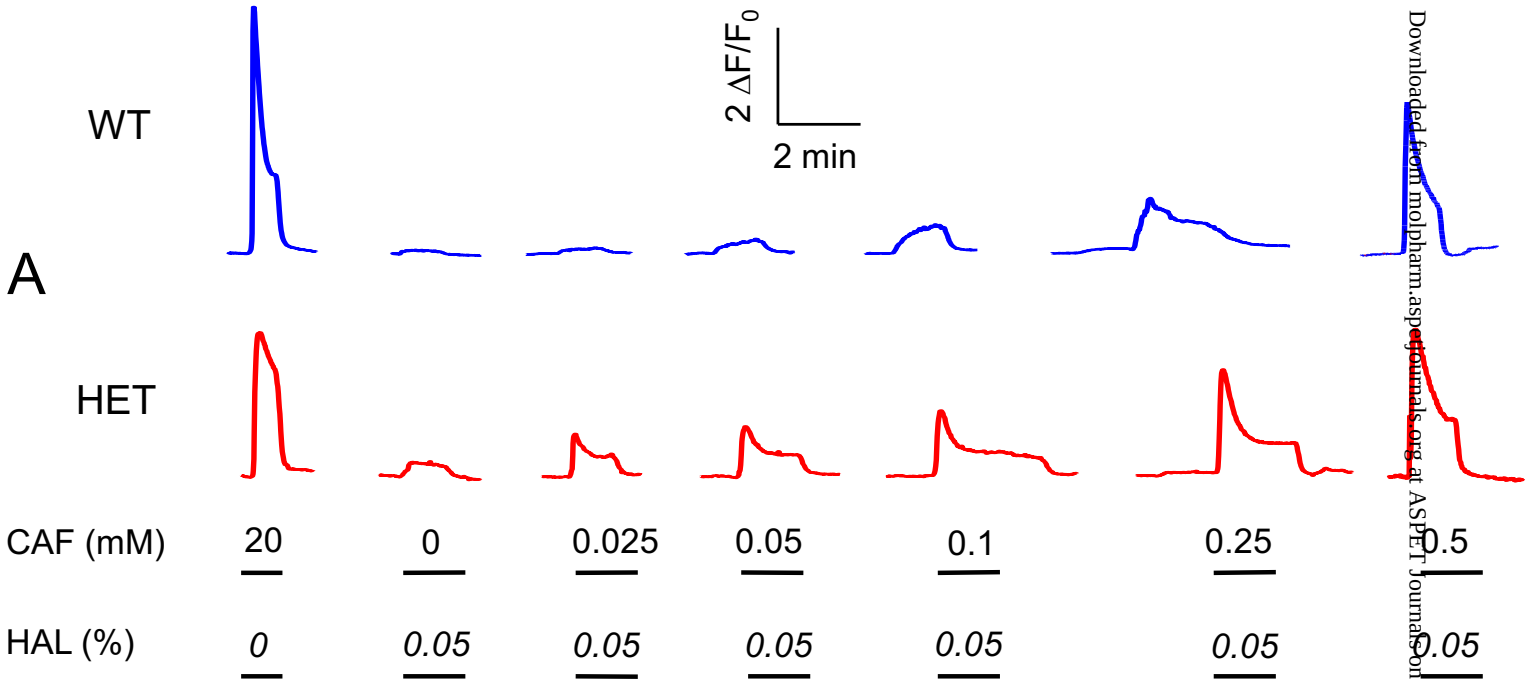

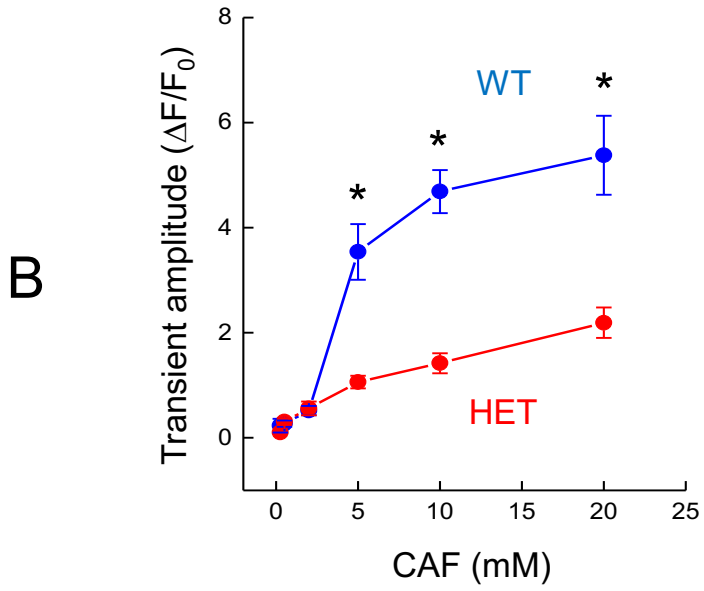

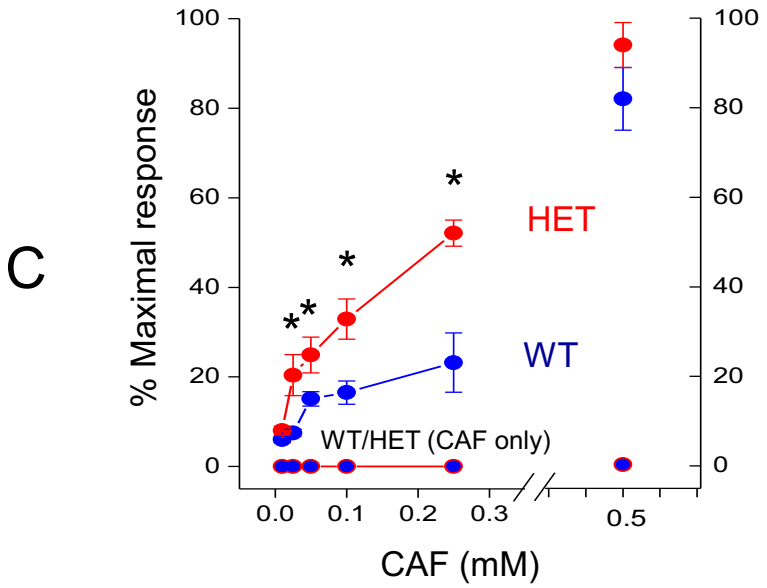

Figure 7